

## Supplementary Methods

### AMS radiocarbon dating

A direct radiocarbon date was obtained for the KC4 maxilla from the Oxford Radiocarbon Accelerator Unit (ORAU) in 1989. It yielded a result of  $30,900 \pm 900$  (OxA-1621). This determination appeared initially to fit within the period expected at that time for the dispersal of modern humans. A renewed dating programme at Kent's Cavern was spurred by the increasing realisation of problems with many of the existing corpus of AMS determinations from the Middle to Upper Palaeolithic of the British Isles on bone dating prior to 30,000 BP<sup>1,2</sup>. The original radiocarbon date for KC4 was considered potentially problematic due to the presence of trace water-soluble glues on the surface of the sampled bone, and the possibility that some of that had remained despite the chemical pre-treatment process<sup>2</sup> (below, we identify this as an animal-based protein glue, which may explain the younger age obtained in 1988, as shown in the main paper). In addition, repeated dating of samples of bone from other sites using an ultrafiltration procedure had suggested that many determinations obtained in the 1980s and 90s and earlier might be underestimating the real age<sup>1</sup>. Further radiocarbon determinations for animal bones from Trenches B and C at Kent's Cavern (excavated between February 1926 - May 1928) were therefore obtained to explore this possibility further and to build a confident chronology for this, and other sites in the British Isles<sup>1,2</sup>.

### Radiocarbon and chemical pretreatment methods

Bone was prepared using methods applied at the ORAU, University of Oxford, UK<sup>1,3,4</sup>. This method utilises a final ultrafilter step<sup>5</sup>, which has been shown to improve the reliability of the ages obtained by the more effective removal of low molecular weight contaminants. Radiocarbon ages are given as conventional ages BP<sup>6</sup>. A new bone-specific background correction has recently been applied to all determinations of bone measured at the ORAU<sup>7</sup>, and this correction has been used in this paper to improve corrections for samples of very small collagen (down to ~5 mg collagen). All of the samples obtained for our study were sampled from collections housed in the Torquay Museum, Torquay, UK (Table S1). A suite of analytical methods was applied to assess the quality of the bone collagen extracts. These included C:N atomic ratios, %weight collagen, %C on combustion, %N and stable isotopic values.

The results from bones obtained both above and below the original find spot (see Table S1) of the maxilla confirmed our suspicion that, if we accept that the maxilla was in its original context in the sequence, the original AMS date was almost certainly too young.

To explore this further, permission was obtained from Torquay Museum to obtain a small sample of dentine from the right P3 of the KC4 specimen for another direct date. The tooth was extracted from the maxilla and carefully sampled at the ORAU so that the external hole could not be seen from the exterior once the tooth had been replaced. Only 89 mg could be drilled due to the small size of the tooth. This produced 0.4% collagen after ultrafiltration pre-treatment, but the total amount extracted was too small for a reliable AMS measurement, so the sample was not dated (Table S2).

Bayesian modelling

The new radiocarbon determinations we obtained (Table S2) were used to construct a Bayesian model to attempt to place the KC4 find within its most likely age. OxCal 4.1 software<sup>8</sup> and the new INTCAL09 curve<sup>9</sup> were used. Bayesian modelling enables the relative stratigraphic information gleaned from the site during the excavation to be incorporated formally along with the calibrated likelihoods. One of us (R. Jacobi) obtained the precise location and depth of the bones that were dated at ORAU from information in the *Kent's Cavern Journal (1926-1932)*. This relative sequence information obtained from the depths of the dated bones below the level of the Granular Stalagmite at the site was used in the age model.

The model consists of a sequence of individual radiocarbon dates (Table S1) and groups of dates in phases running from the bottom (20'-0 (6.09m) below the granular stalagmite) to the top (3'-4'-0 (0.91-1.21m) below the stalagmite). In some parts of the model there is uncertainty about the relative age. In the lowest parts, for instance, there is a possibility that Middle and Upper Palaeolithic material may be present at overlapping depths in the two excavated trenches<sup>2</sup>. A flint blade was excavated at 15'-0 (4.62 m) for instance, whilst adjacent to this in trenches excavated in 1934-1938 Middle Palaeolithic artefacts were found at depths between 13'-9" (4.24m) and 17'-6" (5.36m). The same Granular Stalagmite was used to measure depth. This may be the reason why between 13'-3" (4.05m) and 15'-0 (4.62 m) we have several older than expected results. Due to this uncertainty we grouped determinations in our model between 12'0"-13'0" and 15'0" into a single phase, in which no relative ordering was inferred. We are confident that the bones themselves do, however, securely pre-date the maxilla. In addition, OxA-14714

(19-20") provides additional information since it is below any artefact, and it therefore acts as a *terminus post quem* for human presence in this part of the site. The upper parts of the sequence (above 7'3") may have been affected by cryoturbation or transport, judging by an analysis of the artefacts, so modelling is potentially problematic. We built two different models with slightly different prior constraints to explore the influence of this possible cryoturbation on our results. One model (Model 1) incorporated all determinations in the upper part of the sequence in their inferred sequence order, whilst a second (Model 2) placed all upper determinations in an unordered phase. Model 1 is a more accurate representation of the archaeology, but assumes reduced significant post-depositional mixing, whereas Model 2 is a more cautious assessment, assuming that mixing is more likely and that there is no constraint imposed in terms of relative ordering.

Posterior probability distributions and an outlier detection analysis<sup>10</sup> were used to assess outliers in the model. This showed two outliers of significance (Figure S1). One of these was OxA-14715 (100% probability of being an outlier). This sample comes from the area where there is some overlap of Middle and Upper Palaeolithic material. The other outlier is OxA-13456 (96% likely to be outlying) from C5'-9" depth. There are two possible explanations. First, we identified some thin glue on the surface of the bone which might not have been removed completely by the solvent pre-wash applied. Second, the bone might be intrusive and affected by cryoturbation processes. On the current evidence we cannot favour either of these two explanations.

We used the **Date** function in OxCal to calculate a probability distribution function (PDF) for the likely age of the human maxilla given its assumed position within the sequence and tested the sensitivity of this distribution to the two models we ran. In Figure S2 we show the PDFs for the age of the maxilla derived from both. There is a large degree of overlap but the PDF for Model 1 (sequence model) appears slightly earlier than that for Model 2. We favour the Model 1 PDF as mentioned above. This PDF corresponds to a range between 43,110—41,890 (68.2% prob.) and 44,180—41,530 (95.4% prob.) in cal BP with respect to INTCAL09 (Figure S2). We compare the data against the NGRIP  $\delta^{18}\text{O}$  record<sup>11</sup>. We used the tuned Greenland-Hulu U/Th timescale<sup>12</sup> for this comparison. The PDF fits at the very end of GIS 11 on this timescale, although we must be careful in comparing these records at this preliminary stage of radiocarbon calibration in the last Glacial and when we are not yet sure of synchronicity or asynchronicity between diverse climate records and locations. When the PDF is compared against similarly modelled distributions for other sites dating to the early expansion of the Aurignacian in western Europe, there is a some similarity, but because the PDF overlaps with dates from latest Neanderthal sites and there is no lithic assemblage in confident association with the maxilla, we are not able to diagnose its cultural affiliation. The age inferred is also significantly earlier than the deposition of the Campanian Ignimbrite, which seals beneath it early Upper Palaeolithic industries in Italy, Greece and Russia<sup>13</sup>.

## Tooth Morphology

### 1. Measurements - Methods, and Sources of Comparative Material

All of the new measurements of the KC4 teeth shown in Table S3 were taken from CT-scans. Definitions used for mesiodistal and buccolingual crown diameters, crown height and root length are those of Moorrees (1957)<sup>14</sup>, and those for root robusticity and root trunk length are as defined in Compton and Stringer<sup>72</sup>. Cervical measurements are those defined by Hillson *et al* (2005)<sup>15</sup>. Measurements made by Keith<sup>16</sup> and Frayer<sup>21</sup> are also shown<sup>16,17</sup>. It can be seen that the dimensions have increased due to the cracks in the specimen enlarging.

Estimates have been made of the corrections that should be applied to the mesiodistal measurements to allow for interstitial wear, using the method of Wood and Abbott<sup>18</sup>: -

Canine: 0.2 mm

Premolar: 0.4 mm

Molar: 0.8 mm.

Crown area and crown index figures have been calculated using the corrected mesiodistal measurements. Both the premolar and the molar are worn beyond the level of maximum convexity on the lingual side. Consequently, the buccolingual dimension will have been reduced and the amount of this cannot be estimated. The result is that the calculated crown area and crown index figures are both lower than they would have been on the unworn teeth.

Comparative crown dimensions for the Mid Pleistocene site of Atapuerca-SH in Spain<sup>19</sup>, the early Neanderthal site of Krapina in Croatia<sup>20</sup>, a sample of European late Neanderthals<sup>21</sup> (Palomas measured by ET), European Early Upper Palaeolithic *Homo sapiens* (<sup>21,22,23,24</sup> Muierii measured by ET) and Recent Europeans<sup>25</sup> are given in Table

S4. The crown measurements of KC4 made by Keith<sup>16</sup> (corrected) are used for comparison, since these were made on the specimen when it had the fewest cracks. Comparative cervical dimensions for Neanderthals (including Krapina) and Upper Palaeolithic (early and late) *H sapiens* (measured by SH and CF and those for Gough's Cave re-measured by TC) are given in Table S6. The samples include teeth from Palomas and Muierii (measured by ET).

Tables S9 and S10 show comparative measurements for root robusticity and root length.

Sources of measurements are: -

- Root Robusticity: '*Sinanthropus*' and recent, Weidenreich (1937)<sup>26</sup>; Atapuerca-SH and Krapina, measurements made by TC on casts in the collection of the Natural History Museum, London; Neanderthals, Genet-Varcin<sup>27,28</sup>, Lumley-Woodyear<sup>29</sup>, Martin<sup>30</sup>, McCown and Keith<sup>31</sup> and NESPOS Database (2010)<sup>32</sup>, Palomas measured by ET; Upper Palaeolithic *H sapiens*<sup>33,17</sup>, Ohalo (cast) and Gough's Cave measured by TC.
- Root Lengths: Gran Dolina Hominid 1<sup>34</sup>; '*Sinanthropus*'<sup>26</sup>; Atapuerca-SH, measurements made by TC on casts in the collection of the Natural History Museum, London; Neanderthals and Upper Palaeolithic *H sapiens*<sup>35</sup>; Předmostí<sup>36</sup>; Recent Europeans<sup>25</sup>. Length measurements are quoted for the lingual, or only, roots measured of '*Sinanthropus*' upper first molars.

## 2. Comparative material for morphology

Sites included in the samples for comparison, and references, are given in Table S11.

'Casts' refers to casts in the collection of the Natural History Museum, London. Krapina

is separated out from other Neanderthals in the tables with the exception of those for cervical measurements and root lengths but, where Neanderthals are mentioned below, this can be taken to include Krapina unless stated otherwise.

A comparative sample of recent human teeth comes from the Iron Age site of Poundbury (Dorset, England) (in the collection of the Natural History Museum, London). Study of root morphology is limited, in the main, to sites that are in the NESPOS Database (2010)<sup>32</sup>, X-ray photographs of Krapina teeth<sup>37</sup>, and those for which there are pictures in the literature. Consequently, there are few Upper Palaeolithic *H. sapiens* teeth to which comparisons can be made (Parpalló, Mladeč, Abri Pataud, Gough's Cave). As with root morphology, the study of endodontic morphology is limited to sites that are in the NESPOS Database<sup>32</sup> (those for which micro CT-scans are available, including the Late Upper Palaeolithic site of Gough's Cave) and those for which X-ray photographs are available – Krapina<sup>37</sup>, Grotta Taddeo (from x-ray photographs kindly provided by R L Tompkins), Parpalló<sup>38</sup> and a small sample of recent teeth<sup>39</sup>. Descriptions for recent teeth are taken from van Beek<sup>40</sup> and Wheeler<sup>39</sup>.

### 3. Descriptions of Traits

#### Trait 1 Canine tuberculum dentale small or absent

Neanderthal upper canines generally have a prominent tuberculum dentale<sup>31,41</sup>, but in some it is slight or absent (e.g. Hortus 9, La Quina 21, La Suard 34, Krapina 6E and D76). It is also present on Archaic *H sapiens* teeth from Skhūl and Qafzeh, and Upper Palaeolithic (Early Modern) teeth from Mladeč and Dolní Věstonice (see Table S12), and can be found on recent human teeth but is usually less prominent. The shape and



degree of convexity of the lingual surface of the KC4 canine is similar to teeth on which the tuberculum dentale is small or absent.

Trait 2 Mild vertical convexity of buccal side of canine root (Figure S3)

Bilsborough and Thompson<sup>42</sup>, in describing the Le Moustier 1 dentition, identify the combined labial contour (crown and root) of Neanderthal anterior teeth as being vertically convex. In most of the Neanderthal upper canines studied there is pronounced vertical convexity of the buccal side of either the entire root (predominantly the case at Krapina), or the apical half of the root, (frequently such that the apex of the root is lingual to the vertical axis of the tooth). In the Upper Palaeolithic *H sapiens* sample the buccal side of the root is mildly convex, as with KC4, or straight. Some of the Neanderthal teeth also have only mild convexity (e.g. four at Krapina and one at La Chaise [Bourgeois-Delaunay 16]) (See Table S12). In addition, in approximately half the Neanderthal teeth the root apex is angled sharply lingually, unlike KC4. This does not generally occur in recent teeth, nor in the Upper Palaeolithic teeth.

Trait 3 Vertical grooves on canine root shallow and narrow (Figure S3)

Patte<sup>43</sup> describes the Neanderthal upper canine root as being mesiodistally flattened, with prominent mesial and distal grooves. The recent modern root form, on the other hand, is normally more conical (or triangular, with mesial and distal flattening and broad buccally), though it also can be flattened. The degree of mesial and distal vertical grooving or ‘infolding’ provides some distinction between Neanderthals and Upper

Palaeolithic *H sapiens*. The vertical grooves on all the Neanderthal teeth studied are wide and deep but mesial and distal grooves are not always both present. The grooves on the Upper Palaeolithic teeth and recent teeth are generally narrower and shallower, as are those on KC4.

Trait 4 No buccal or lingual dentine spurs apical to cervix in canine or P<sup>3</sup> pulp chambers (Figure 1d)

Kallay<sup>44</sup> describes the shape of the pulp chambers of Krapina canines as being predominantly ‘lancet’ shaped due to a narrowing of the root canal just below (apical to) the cervix, as seen in mesial/distal view, caused by the presence of buccal and lingual dentine spurs. These are also found in all of the other seven Neanderthal upper canines studied, though in the Le Moustier juvenile they are faint. There is no trace of these in the KC4 canine and the Gough's Cave canines have a widening of the root canal in this position. Kallay<sup>44</sup> states that the lancet form is only occasionally indicated in recent teeth and it is not described by van Beek<sup>40</sup> or Wheeler<sup>39</sup>. The buccal and lingual spurs in the root canal found in canines also occur in a little under half the Krapina and other Neanderthal upper third premolars studied but not in the KC4 premolar nor in the Gough's Cave premolars.

Trait 5 Pronounced lingual narrowing of canine root canal towards apex (Figure 1d)

Seen in mesial view, there is generally a distinct narrowing of the root canal in recent human upper canines at a point one half to two thirds of its length from the cervix. This

narrowing is from the lingual side of the tooth and is particularly pronounced in the KC4 canine. It also occurs in the Gough's Cave canines. The root canal in the Neanderthal upper canines studied tends to taper evenly from the spurs to the apex, though the lingual narrowing is seen to a mild degree in some (e.g. La Quina 21).

Trait 6 P<sup>3</sup> low angle of inclination of occlusal part of buccal surface to vertical axis (Figure S4)

Frequently, the buccal surface of the Neanderthal upper third premolars is more swollen towards the cervix (particularly at Krapina) than is the case in KC4 and in Upper Palaeolithic *H sapiens* teeth, but there is variation in both groups and in both there are teeth with similar convexity to that of KC4. The angle of inclination of the occlusal part of the buccal surface to the vertical axis of the tooth (as indicated in Figure S4) is distinctly greater in Neanderthals than in the Upper Palaeolithic teeth, with little overlap in the range of values found (see Table S13). The KC4 angle is at the lower end of the Upper Palaeolithic range (though this may be partly due to the small amount of the buccal surface remaining).

Trait 7 Small dimensions and characteristic shape of P<sup>3</sup> pulp chamber and root canals (Figure 1b)

The pulp chamber of the KC4 premolar is smaller in both mesiodistal and buccolingual dimensions than in the Krapina and other Neanderthals samples but, as with the canine (Trait 22), the maximum mesiodistal dimension is proportionally smaller than the

maximum buccolingual dimension (Table S14). Similarly, the root canal before bifurcation has a mesiodistal dimension below the Krapina and other Neanderthals ranges and the buccolingual dimension at the bottom of the other Neanderthals range. The pulp chamber and root cross-sectional areas are also all well below both Neanderthal sample ranges. This could be partly due to the likely age of KC4. Oi *et al.*<sup>45</sup> found that the mesiodistal width and the height of the pulp cavity decrease with age and also the diameter of the root canals. However, the same applies to the less worn Gough's Cave tooth, in which all the measurements are below the Krapina and other Neanderthals ranges apart from the maximum buccolingual dimension of the pulp chamber, which is at the bottom of the other Neanderthals range. The shape ratios for the KC4 premolar pulp chamber and root before bifurcation (and Gough's Cave pulp chamber) are also below both Neanderthal sample ranges but are within the ranges found in a small sample of recent teeth from Wheeler<sup>39</sup>. However, the two ratios are very similar in KC4, as found in the Neanderthal samples, but unlike the recent teeth, in which the root above the bifurcation is, on average, distinctly narrower than the pulp chamber.

#### Trait 8 Rectangular shape of M<sup>1</sup> occlusally and at cervix

Allowing for the considerable mesial interproximal wear, the occlusal outline of the KC4 molar is near rectangular, with a rounded distal surface and buccal protrusion of the mesiobuccal cusp. The squared shape suggests that there was a large hypocone. Bailey<sup>46</sup> and Gómez-Robles *et al.*<sup>47</sup> identify certain differences in the occlusal shape of upper first molars between Neanderthals and anatomically modern humans. Neanderthal

upper first molars are markedly skewed, with the lingual cusps placed distal to the respective buccal cusps. In addition, they possess a large protruding hypocone, smaller metacone, and cusps that are more internally placed. Lumley-Woodyear<sup>29</sup> describes Neanderthal upper first molars as being trapezoid in shape, and having a buccally protruding paracone, against the parallelogram shape of anatomically modern humans. In relatively unworn teeth the difference in occlusal outline is very clear. The shape of the KC4 upper first molar (i.e. near rectangular) does not conform to the Neanderthal pattern but is alike in shape to many Archaic *H sapiens* and Upper Palaeolithic *H sapiens* upper first molars (e.g. from Skhül, Předmostí, Mladeč, Dolní Věstonice). Hillson *et al.*<sup>15</sup> defined diagonal cervical measurements (distobuccal to mesiolingual and distolingual to mesiobuccal) for molars, which can be used to determine the degree of skewness of upper first molars. TC has taken measurements of upper first molars from five groups (Table S15) (apart from Poundbury and Gough's Cave, taken from casts or using the NESPOS 2010 database<sup>32</sup>) and determined the ratio of the two measurements (distobuccal to mesiolingual over distolingual to mesiobuccal). With the exception of Archaic *H sapiens*, the groups have similar means and minimum ratios but only the Archaic *H sapiens* and recent groups have the very high ratios, as found in KC4, that denote a near rectangular shape (e.g. Skhül 4 in Archaic *H sapiens*).

#### Trait 9 Shape of M<sup>1</sup> pulp chamber polygon (Figure S5)

Table S16 gives the dimensions of the pulp chamber polygons of the KC4 upper first molar and those of three reference samples - Krapina, other Neanderthals and Gough's Cave. The positions of the pulp horn tips were recorded and then linked together at the

level of the pulp horn tip furthest occlusally from the cervix to form a four-sided polygon such that the polygon was in line with the horizontal axis of the tooth. The crown base area was also measured at this level.

With one exception, the values for KC4 are within the range of values found for Gough's Cave, but they differ considerably from the values for Neanderthals: -

- Three of the KC4 polygon angles are out of the other Neanderthals sample range, in particular the protocone and hypocone, and all four are out of range for Krapina and over two standard deviations from the mean (three standard deviations for the metacone and hypocone). There are also differences between the Krapina and other Neanderthals samples, particularly in the metacone angle, where the ranges of values do not overlap. The mean metacone and protocone angles are the same in the Krapina sample but seventeen degrees apart in the other Neanderthals sample. Bailey<sup>46</sup> and Gómez-Robles *et al.*<sup>47</sup> describe the occlusal polygons of Neanderthal upper first molars (formed by linking the four cusp tips) as being skewed compared to anatomically modern humans, with distal displacement of the lingual cusps, leading to higher protocone and metacone angles and lower paracone and hypocone angles. The Krapina and other Neanderthals pulp chamber polygons reflect this, the Krapina polygons being a little more skewed, in the main, than those of the other Neanderthals sample, and the polygons of both being considerably more skewed than those of Gough's Cave and KC4. The less skewed shape of the KC4 and Gough's Cave polygons is also shown by the higher figures for the ratio of the diagonal measurements, the two diagonals being more similar in size in these than in the

Neanderthal samples. There is no overlap in the ranges of values and the lowest Gough's Cave value is four standard deviations from the Krapina mean.

- The relative size of the mesial side of the KC4 polygon, compared to the total circumference, is out of both the Krapina and other Neanderthals ranges, it being proportionally larger. In the Neanderthal samples the means for the relative sizes of the mesial and distal sides are the same but for KC4 and Gough's Cave the mesial side is generally larger. The lingual side is in nearly all cases smaller than the buccal but the difference is more pronounced in KC4 and Gough's Cave, the KC4 value and Gough's Cave mean for the relative size of the lingual side being below the Krapina range. KC4 fits well with the figures for Gough's Cave, only the relative distal length is slightly below the Gough's Cave range of values. (For relative sizes of the sides of occlusal polygons see refs 46 and 47).
- The relative size of the KC4 occlusal polygon area compared to the crown base area is within the ranges of all three reference groups. However, the fact that the relative areas for Gough's Cave are above the Krapina and other Neanderthals means is in line with the fact that the occlusal polygon area in Neanderthals is relatively smaller<sup>46</sup>.

#### Trait 10 No taurodontism in M<sup>1</sup>

Taurodontism in molars (absent in KC4) is a characteristic particularly associated with Neanderthals<sup>48</sup> and is widespread amongst later Neanderthals, but there are some sites at which it is not present. These include Biache (studied by CS), the Ehringsdorf adult (Virchow 1920 quoted in Ref 26), Bourgeois-Delaunay<sup>49</sup>, Bau de l'Aubesier 11<sup>50</sup> and

the Pesada upper third molar<sup>51</sup> from the later Middle Pleistocene, and Zafarraya 2<sup>52,53</sup>, Valdegoba 1<sup>54</sup> and Cova del Gegant<sup>55</sup> from the Late Pleistocene. In addition, not all the Krapina molars exhibit taurodontism<sup>56</sup>. Taurodontism is rare in Upper Palaeolithic *H sapiens* and recent teeth<sup>38</sup>.

#### Trait 11 Low robusticity of P<sup>3</sup> root

Table S9 shows comparative measurements for root robusticity. Weidenreich<sup>26</sup> describes a decrease in root robusticity between ‘*Sinanthropus*’ teeth and recent teeth. The root robusticity figures of the KC4 canine and the molar are above the means for recent teeth and within the ranges for Neanderthals. The figure for the premolar, though, is distinctly smaller, below the mean for recent and below the Krapina and other Neanderthals ranges. All three teeth are in range when compared to the Upper Palaeolithic *H sapiens* sample. Of the three teeth, the greatest reduction in root robusticity between Neanderthals and Upper Palaeolithic is seen in the premolar.

#### Trait 12 Small actual and relative cervical dimensions of P<sup>3</sup>

Comparative cervical dimensions for Neanderthals (including Krapina) and Upper Palaeolithic (early and late) *H sapiens* are given in Table S6. As with the comparative crown dimensions (see Table S4), the Neanderthal mean length and breadth dimensions, with the exception of the upper first molar breadth, are all greater than those of the Upper Palaeolithic sample and this is most notable in the breadth of the upper third premolar. The Upper Palaeolithic upper first molars are more rectangular than the



Neanderthal teeth, resulting in a higher average cervical index figure. The length and breadth of the KC4 canine are both near the Neanderthal means but they are also both within the ranges for the Upper Palaeolithic. In contrast, the breadth of the KC4 premolar is at the bottom of the Neanderthal range, and the length is below range and over two standard deviations below the mean. The cervical area figure for this tooth is also below the Neanderthal range. The length of the KC4 molar is between the Neanderthal and Upper Palaeolithic means but the breadth is at the top end of the Neanderthal range, and nearer the Upper Palaeolithic mean. Consequently, the index figure is above the mean for Neanderthal and near equal to that of the Upper Palaeolithic.

In Table S7 the relative sizes of the mesiodistal and buccolingual cervical dimensions of the three teeth compared with each other are given for the Neanderthal and Upper Palaeolithic samples and KC4. As with the crown dimensions, the cervical buccolingual dimensions of the canine and premolar are proportionally larger compared to the molar in the Neanderthal sample than in the Upper Palaeolithic sample (particularly the premolar), and this is also the case with the mesiodistal dimensions. In contrast, the length and breadth of the canine are proportionally larger compared to the premolar in the Upper Palaeolithic sample. The relatively small cervical dimensions of the KC4 premolar in relation to the canine and molar can be seen, with three out of four comparative figures being outside the Neanderthal range and two standard deviations or more from the mean.

The KC4 premolar is therefore small, both actually and in relation to the canine and the molar, compared with Neanderthal teeth, being almost always outside the ranges of

values found in this sample. Conversely, it is within the ranges found in the Upper Palaeolithic sample, both in itself and in relation to the other teeth.

#### Trait 13 Relative cervical and crown dimensions of canine and M<sup>1</sup>

In Table S8 the cervical measurements are compared to the crown measurements for the same teeth. Sources for the crown measurements are as for Table S6. It can be seen that the cervical measurements for length are proportionally greater in the Upper Palaeolithic *H. sapiens* sample. The ratios for KC4 premolar and molar breadth are higher than they would have been on the unworn teeth. The canine length ratio is above the Neanderthal range but within the Upper Palaeolithic range and the breadth ratio is at the top of the range for both Neanderthal and Upper Palaeolithic (and over two standard deviations above the mean for Neanderthal) but the third premolar length ratio is below the range of both comparative samples. The molar breadth ratio is two standard deviations above the Neanderthal mean and above range.

#### Trait 14 Possible tubercle extensions on canine (Figure S6)

The two lingual inroads of enamel onto the worn occlusal surface of the KC4 canine suggest an irregular lingual morphology of the crown. These could be the remnants of medial and distal fossae, both of them distal to a prominent mesially placed tubercle extension and either side of a smaller narrow distally placed tubercle extension, with possibly another tubercle extension distal to this (mesial tubercle extension/ site of mesial tubercle extension indicated by arrows in Figure S6).

Hillson and Coelho<sup>52</sup> point out that tubercle extensions on upper canines are uncommon on recent human teeth, and are not found on the Dolní Věstonice or Pavlov early modern upper canines, but are seen on the upper canines of the Hortus 3 Neanderthal and the Lagar Velho Child. They are common amongst Neanderthals, occurring on almost all the Krapina upper canines (the mesially placed extension tending to be the most prominent) and in nearly eighty per cent of the Neanderthal (excluding Krapina) sample (see Table S12). They are less common on Upper Palaeolithic *H sapiens* specimens, occurring in under half the sample, and when they do occur they tend to be finer. Their rate of occurrence on Archaic *H sapiens* upper canines is similar to that found in Neanderthals. The more frequent form of the lingual surface in both Upper Palaeolithic and recent humans is to only have a central buttress, with or without a tuberculum dentale.

Trait 15 Irregularities in sides of root canals, especially in the canine

The irregularities seen in the sides of the root canals (variations in their width) in the KC4 teeth, particularly the canine, are as found in Krapina teeth<sup>44</sup>. These were considered to be a Neanderthal trait and not generally found in anatomically modern human teeth. The irregularities occur in all the upper canines in the non-Krapina Neanderthal sample but only in one upper third premolar and one upper first molar. In addition to all the upper canines they also occur in some, but not all, Krapina upper third premolars. This feature is seen in a mild form in the Gough's Cave canines.

Trait 16 Greater lingual inclination of M<sup>2</sup> lingual root than is found in M<sup>1</sup> (Figure S7)

Weidenreich<sup>26</sup> compares the shape of the lingual roots of *Sinanthropus* upper first and second molars, which are straight and pointed lingually, with recent humans, in which they curve buccally so that the apices are near vertical (though this is not always the case). The Neanderthal La Quina second molar roots are seen as intermediate. However, the Neanderthal first molar lingual roots tend to be similar in shape to recent humans and in some the entire root is near vertical. At Krapina the lingual roots of upper first and second molars both appear near vertical but at La Quina the second molar root is directed more lingually than that of the first molar (Martin 1923) and the same is the case at Le Moustier, Spy (2), Amud (1) (Sakura 1979) and St Césaire (cast). In recent humans the lingual root tends to be less lingually inclined in the second molar than in the first, the reverse of the above. The lingual roots of both the first and second Kent's Cavern upper molars are near straight (the shape of the second molar roots being observable from the remains of its root socket), and the lingual inclination of the second molar lingual root is quite distinctly greater than the first, similar to La Quina. In contrast, the lingual roots of the Gough's Cave specimens are of recent human form.

Trait 17 Crown dimensions and root lengths lie in both Neanderthal and modern human ranges

It can be seen in Table S4 that the mean length and breadth crown dimensions for Late Neanderthal and Early Upper Palaeolithic *H sapiens* are similar, apart from the breadth measurement for the upper third premolar, which is substantially lower in the Early Upper Palaeolithic. The KC4 measurements fall within range and, in most cases, within

one standard deviation of the mean, for both Late Neanderthal and Early Upper Palaeolithic but, apart from upper first molar breadth, below range for Krapina. The premolar and molar measurements that are over one standard deviation below the mean for Late Neanderthal (premolar breadth) and Early Upper Palaeolithic (molar crown index) are ones that have been reduced due to wear. The canine length is a little over one standard deviation below the mean for both samples. The crown index of the canine is at the upper end of the range for Early Upper Palaeolithic but well within the much greater range found in Late Neanderthal teeth. In Table S5 the relative sizes of the mesiodistal and buccolingual dimensions of the three teeth compared with each other are given for the Late Neanderthal and Early Upper Palaeolithic samples and KC4. The results are not conclusive. The buccolingual dimensions of the canine and premolar are proportionally larger compared to the molar in the Late Neanderthal sample than in the Early Upper Palaeolithic sample, with the KC4 dimensions intermediate in both cases. The other ratios are near identical in the two samples. The relative size of the buccolingual dimension of the canine compared to the premolar and the molar would be lower in the unworn teeth. This could bring the ratio for the canine compared to the molar to the bottom of the range of values found in the Late Neanderthal sample. The relatively small mesiodistal dimension of the KC4 canine can be seen in relation to both the premolar and the molar.

Weidenreich<sup>26</sup> describes a decrease in root length between '*Sinanthropus*' teeth and recent teeth. In the upper teeth this is least pronounced in the molars, compared with a worldwide sample of recent teeth, and most pronounced in the canine. In Table S10 it can be seen that the KC4 canine root length lies at the bottom of the range for Neanderthals (within two standard deviations of the mean) but it is above the range for

Upper Palaeolithic, as is the length of the molar lingual root. However, the Upper Palaeolithic sample size is necessarily small, and both the canine and molar root lengths are within the range for recent European. They are also within the range of values published for the Upper Palaeolithic site of Předmostí. That for the premolar lies in both the Neanderthal and Upper Palaeolithic ranges. Bailey<sup>35</sup> found the root lengths of the upper incisors and canine to be particularly diagnostic in differentiating between Neanderthal and Upper Palaeolithic anatomically modern humans.

Trait 18 Canine angle of inclination of occlusal part of buccal surface to vertical axis

The shape of the buccal surface of the KC4 canine, as seen mesially, (mild convexity at the cervix and then a lingual inclination) occurs in all the samples, and in some the cervical part is vertical, without any curvature. However, in two thirds of the Neanderthals the inclination of the buccal surface commences at the cervix. The angle of inclination of the occlusal part of the buccal surface to the vertical axis of the tooth (from the point of maximum convexity) is similar in the Neanderthal and Upper Palaeolithic *H sapiens* groups, and the angle found in the KC4 canine lies within the ranges found in both (Table S13).

Trait 19 Mesiobuccal bulge in occlusal outline of canine but not of P<sup>3</sup>

The mesiobuccal bulge (tuberculum molare) seen in the occlusal outline of the KC4 canine is common in all five samples but least so in the Upper Palaeolithic *H sapiens* sample (see Table S12).

The occlusal outline of the KC4 premolar is symmetrical, with no sign of a mesiobuccal bulge. This feature is more common in Neanderthals than in Upper Palaeolithic *H sapiens* upper first premolars, only two instances being found in the Upper Palaeolithic sample (see Table S12). Lumley-Woodyear<sup>29</sup> and Patte<sup>43</sup> state that it is very rare, and when present only faint, in recent humans, and it was not found in the Poundbury sample.

#### Trait 20 Canine root surface smooth

Patte<sup>43</sup> and Lumley-Woodyear<sup>29</sup> refer to the granulated appearance of some Neanderthal upper canine roots and this is observed in over half the Neanderthal sample (excluding Krapina) but not in the Krapina teeth. It is not seen in the Upper Palaeolithic *H sapiens* sample, nor in KC4 (see Table S12).

#### Trait 21 Single rooted P<sup>3</sup>

The upper third premolar has evolved from being predominantly two-rooted in early hominins to being frequently single-rooted in recent humans. In Irish and Guatelli-Steinberg's (2003) pooled samples of robust and gracile Plio-Pleistocene fossil hominins, all the robust hominins had two or more roots on upper third premolars and 93.8% of the graciles. In recent humans, 42.3% of Europeans have two-rooted upper third premolars and in present day populations this figure varies between 4.9% and 68.4%<sup>57</sup>. The Neanderthals predominantly have two-rooted upper third premolars but this is also frequently the case with early Upper Palaeolithic modern human

specimens<sup>58</sup>. All of the Krapina upper third premolars are two-rooted, and all fourteen of the other Neanderthal examples that can be determined have at least two roots, only Tabun 1 being reported as having a single root<sup>31</sup>. Nine Upper Palaeolithic specimens with at least two roots were noted. Single-rooted Upper Palaeolithic upper third premolars are reported for Mladeč 2<sup>59</sup>, and Gough's Cave 87-29 and observed in Gough's Cave 87-139. Coppa *et al.*<sup>60</sup> define a modern human Palaeolithic-Mesolithic dental morphological complex for Europe (Italy, France, Croatia, Czech Republic and Slovakia) that includes a high frequency occurrence of two-rooted upper third premolars. KC4 is unusual in having a single root when compared with either population.

#### Trait 22 Dimensions of canine pulp chamber

The pulp chamber and root canal measurements of the KC4 canine are compared with four reference groups in Table S14. The measurements of the reference groups mostly overlap but the Gough's Cave pulp chamber and root canal cross sectional areas and maximum root canal mesiodistal widths are all below the ranges of values for Krapina. The mesiodistal widths of the Krapina and other Neanderthals pulp chambers and root canals are all greater than is found in KC4, whereas the buccolingual width ranges overlap, leading to lower (narrower) shape ratios in KC4. The KC4 measurements are proportionally similar to Gough's Cave but are all below the Gough's Cave ranges of values. The level of occlusal wear in KC4 indicates that it is likely to have belonged to an older individual than is found in the reference material, and the reduced dimensions may be due to the deposition of secondary dentine<sup>61,62</sup>.



### Trait 23 Height of P<sup>3</sup> pulp chamber roof relative to cervix

In recent upper premolars the roof of the pulp chamber between the two pulp horns in the third premolar is generally (but not always) distinctly occlusally placed in relation to the cervix, whereas in the fourth premolar it is at a similar level<sup>40</sup>. Despite the level of wear on the KC4 upper third premolar, the roof of the pulp chamber is further from the cervix than is found in the two Neanderthal samples (Table S14). It is also further than is found in Gough's Cave 87-139. The distance from the roof of the pulp chamber to the bifurcation of the roots in KC4 is within the ranges found in the Neanderthal teeth and within one standard deviation of the mean in a sample of recent teeth<sup>63</sup>. (There is only a single root canal in the Gough's Cave premolar).

*Note: In studying the teeth from Krapina, tooth identifications and groupings into 'Krapina Dental People' are taken from Ref 64. Teeth 166 and 177 were identified as upper first molars instead of upper second molars, as recommended by Trefny<sup>65</sup> and, in addition, tooth 176 was also identified as an upper first molar instead of an upper second molar and teeth 58 and 178 were identified as upper second molars instead of upper third molars (both have distal interproximal facets).*

CT study and reconstruction

MicroCT study and reconstruction

MicroCT scanning of the maxilla was undertaken with an X-Tek HMX160  $\mu$ CT system (X-Tek Systems Ltd, Tring, UK). The specimen was placed on a small piece of polystyrene foam mounted on the scanner turntable, which was rotated through  $360^\circ$  in 1567 steps (*i.e.* with an angular increment of  $0.23^\circ$ ) with a 2D image collected at each step. Extraneous noise in the images was minimised by taking 64 images at each scanning step and averaging the results. The X-ray source used a scanning voltage of 79 kV, a current of 16  $\mu$ A, a 0.1mm copper filter and an aperture setting of 75%. Image reconstruction, to convert the 1567 images into a 3D volumetric structure, was performed using NGI CT Control software (X-Tek Systems Ltd, Tring, UK) and applying a Butterworth filter. The volume consisted of  $1000 \times 1000 \times 500$  voxels with a voxel size of  $49.1 \times 49.1 \times 98.2$   $\mu$ m. From this volume a stack of 500 16-bit tiff (Tagged Image File Format) images was exported (also  $1000 \times 1000$  pixels) and imported into AMIRA 4.1.1 (Mercury Computer Systems Inc., USA) for image segmentation and further analysis.

A virtual 3D model of the specimen was created by a combination of thresholding and manual segmentation. The thresholds for separating bone and teeth from the surrounding air were determined by using the half maximum height protocol<sup>66</sup>. Following this protocol, the half maximum height was calculated as the mean of the minimum and maximum grey values along a row of pixels that spanned the interface between bone and air in a CT slice. In order to account for the slightly higher density of the dental tissue, the half maximum height values for the alveolar bone and the teeth were calculated individually. The final thresholds were then determined as the mean maximum height values for several randomly selected slices. Due to the overlapping

density ranges of dentine and alveolar bone, some manual segmentation was required to separate the tooth roots from the alveolar sockets. In addition, the adhesive that held the bone fragments and teeth together was separated manually from the surrounding bone.

The resulting 3D model was used for visual exploration and quantitative analysis of the specimen. Longitudinal sections through the teeth allowed the pulp chambers and root canals to be studied, while making the model transparent provided a 3D visualisation of these cavities within the teeth. Measurements of the tooth dimensions were taken based on the 3D surface model as well as longitudinal and cross-sections through the teeth.

During earlier examination of the original specimen, doubts had been raised as to whether the first reconstruction, during which the preserved premolar was glued into the P<sup>4</sup> socket, was correct. The virtual model provided a non-invasive approach to this problem, allowing the premolar to be extracted and repositioned accordingly. With the original reconstruction of the alveolar bone, it was found that the premolar did not fit into the P<sup>3</sup> socket since it collided with the distal wall of the socket. However, closer inspection of the alveolar bone in the 3D model with transverse CT images revealed that the distal wall of the P<sup>3</sup> socket is part of a fragment, which had been glued to the specimen in a displaced position (Figure S8). The buccal surface of the fragment was not in line with the better preserved alveolar bone around the M<sup>1</sup>. Therefore, the fragment was also separated virtually, rotated and repositioned. This correction resulted in a better fit of the premolar into the P<sup>3</sup> rather than the P<sup>4</sup> socket (Figure S9), suggesting that it was indeed in the wrong position.

In addition, there are morphological reasons for the reattribution of the premolar from P<sup>4</sup> to P<sup>3</sup> and these are listed in Table S17.

### Reconstruction of the maxilla

Following the virtual reconstruction of the maxilla it was decided to physically reconstruct the specimen and move the premolar to its newly identified P<sup>3</sup> socket from the current P<sup>4</sup> socket. To undertake this, it was necessary to deconstruct the whole maxilla, which meant detaching the units of the jaw, premolar and canine teeth. The decision was then made to separate out the two teeth and individual units of the jaw and to then reconstruct the maxilla following the best fit from the virtual reconstruction.

### Condition prior to restoration work

The maxilla is in a fragile but stable condition. The surface of the molar (which sits unadhered in its socket) is cracked but shows no signs of further environmental deterioration. The premolar and canine teeth are stable and show no signs of deterioration, but had been adhered into place with a yellowing adhesive that had also coated the sides of the teeth. The maxilla was adhered together (Figure 1a) using the same adhesive. The adhesive that had been used to adhere the fragments of maxilla and teeth together was yellowing and slightly brittle, with signs of shrinkage along the joints between the bone fragments and teeth.

Samples of the adhesive were removed and spot tested for identification<sup>67,68</sup>. Following a range of tests, the adhesive was identified (using the Biuret Test for proteins) as an animal glue of unknown origin but dating from the original restoration of the maxilla. The same glue had been used to adhere the premolar, canines and fragments of the maxilla into place.

#### Testing for solubility of glue prior to detachment of units

A 0.05g sample of the glue was taken to assess the glue solubility. Three small samples were placed on glass slides and each was tested using ethanol and cold and warm deionised water. Samples were identified as being soluble in warm water at approximately 40°C. No sample was soluble in ethanol. It was therefore decided to disarticulate the jaw components using deionised water heated to 40°C.

The first stage of the process was to remove the glue that had been used to adhere the jaw units together and to then dismantle the jaw into its individual units. The animal glue was softened at each joint around the tooth using the warm water and each joint was separated. The warm water was applied with a wood splint wound with a small amount of polyester gauze wrapped onto its end. The moisture content of the gauze was kept to a minimum to reduce the amount of water that was applied to the bone. Once softened the glue was removed by gently swabbing the joints until the units of the maxilla detached. Thicker lumps of the glue were removed with a fine scalpel blade. Once detached, any remaining glue was removed from the surface and joint of the bone units in the same way. All glue was removed from the teeth using the same method until

no glue could be seen to discolour them under UV light or under microscopic inspection at 200x magnification.

Once all excess and surface glue was removed, the teeth and bone units were laid out on Mylar™ and air dried under ambient environmental conditions.

The individual units of the maxilla were tacked together using Paraloid B72 Adhesive<sup>69</sup>. As the removal of the premolar tooth from P4 had led to the structural loss of the socket it meant that the socket had to be structurally supported and reconstructed. A small polyethylene (PE) tube drawn to the maximum width of the P<sup>4</sup> tooth socket was tacked into place where the original tooth had been sited. A structural gap fill was then built to support the maxilla in the area where the premolar was originally positioned. The structural gap fill was built with a mixture of glass microballoons and 45% Paraloid B72 Adhesive (dissolved in acetone). Once dried the temporary PE support was removed. The tooth originally in the P<sup>4</sup> tooth socket was then adhered into the existing P<sup>3</sup> tooth socket and the second section of the maxilla and premolar adhered into place (see Fig S9). All adhesion was undertaken with Paraloid B72 Adhesive<sup>69</sup>. A cone of high density polyethylene (HDPE) tubing (shaped to the P<sup>4</sup> socket) was then placed into the P<sup>4</sup> socket to give the object more structural support (see Fig S9). The dimensions and shape of the cone were guided by the CT scans and reconstruction and the HDPE cone was shaped from these images.

Mounting of the maxilla for display

To place the maxilla in its proper position for display a 4 mm Perspex rod was positioned inside the HDPE cone and adhered in place using Paraloid B72 adhesive<sup>69</sup>. This was then mounted into a perspex base.

## Ancient DNA

Genetic analysis of the specimen was attempted using previously described techniques for isolating and amplifying DNA from preserved remains. Because of the high potential for contamination with modern human DNA fragments, extreme care was taken at each step in the DNA extraction and amplification stages. A small (<0.2g) amount of bone powder was collected from the specimen as described above. The powder was transferred to a sterile container and transported to a dedicated ancient DNA facility in Madrid, Spain for DNA extraction. Extraction was as described in Svensson *et al.*<sup>70</sup>. The sample was co-extracted with three Neanderthal specimens, including one from which DNA had been successfully amplified in a different laboratory (positive control), three ancient arctic foxes and one extraction blank (negative control). Following DNA extraction, amplification was attempted of a short fragment of the mitochondrial control region that has been demonstrated to be hypervariable in both modern human and Neanderthals (Krings *et al* 1997). The primers 2320F and 262R<sup>71</sup> were used, and amplification was attempted twice. In both experiments, bands indicating positive amplification were observed only in the previously successful Neanderthal (positive control) and the Kent's Cavern specimen. PCR amplicons from all four positive amplifications were then cloned into competent bacterial cells for standard ABI sequencing using the TOPO-TA kit (Invitrogen, UK) according to manufacturers'

instructions. From the resulting bacterial colonies, 36 were randomly chosen from each of the four successful PCRs for additional PCR amplification and sequencing.

Sequencing was performed on an Applied Biosystems sequencer, using BigDye v 3.0 according to manufacturer's protocols. Analysis of the 72 colonies sequenced from the Kent's Cavern specimen revealed at least 18 distinct mitochondrial DNA sequences, all of which fall within the modern diversity of anatomically modern humans. Because it is impossible to distinguish between endogenous sequences of modern humans and contamination (via excavation, handling, etc.) these results are therefore inconclusive as to the specific identity of the Kent's Cavern specimen. It remains unknown whether the specimen is genetically similar to modern humans, or whether the DNA within the sample was degraded to an extent that no endogenous (Neanderthal or otherwise) DNA was recoverable using these techniques.

### Supplementary Notes

### Acknowledgements

We would like to thank Robert Kruszynski (Natural History Museum, London) for allowing access to fossils and casts in his care and for his kind help. We are grateful to Sue Taft for the CT-scanning of the specimens and to Richie Abel for CTs of comparative specimens. We would also like to thank Marcel Bradtmöller of NESPOS for all his assistance, and the following for making available CT-scans of fossils from Neanderthal sites for viewing on the NESPOS Database: La Chaise de Vouthon – Roberto Macchiarelli and Dr J F Tournepiche of Musée de Angoulême; La Quina –



Roberto Macchiarelli and Dr D Berthet of Musée de Lyon; Le Moustier – Bernhard Illerhaus; Spy – Patrick Semal. In addition we wish to thank Helen Liversidge for providing specimens of modern teeth, Silvia Bello for assistance with using the Alicona microscope, Alfredo Coppa for making available dental morphological data for upper canines, and R L Tompkins for the donation of x-ray photographs of fossil dentitions. Matthew Skinner, Philipp Gunz, Michael Richards, Anthony Olejniczak and Jean-Jacques Hublin also advised on other investigative approaches to the study of the specimen, for which we are grateful. We thank the staff of the ORAU, University of Oxford for their careful laboratory work. Finally we would like to thank Harry Taylor of the Natural History Museum Photography Unit for taking photographs of the Kent's Cavern KC4 specimen.

#### Supplementary references

1. Higham, T.F.G., Jacobi, R.M. and Bronk Ramsey, C. 2006. AMS radiocarbon dating of ancient bone using ultrafiltration. *Radiocarbon*, 48(2), 179-195.
2. Jacobi, R.M., Higham, T.F.G. and Bronk Ramsey, C. 2006. AMS radiocarbon dating of Middle and Upper Palaeolithic bone in the British Isles: improved reliability using ultrafiltration. *Journal of Quaternary Science*, 21(5), 557-573.
3. Bronk Ramsey, C., Higham, T., Bowles, A., Hedges, R. 2004. Improvements to the pretreatment of bone at Oxford. *Radiocarbon*, 46, 155-163.

4. Brock, F., Bronk Ramsey, C., Higham, T.F.G. 2007. Quality Assurance of ultrafiltered bone dating. *Proceedings of the 19th International Radiocarbon conference* (eds : C. Ramsey and T. Higham), *Radiocarbon* 49(2): 187-192.
5. Brown T.A, Nelson D.E, Vogel J.S and Southon J.R. 1988. Improved collagen extraction by modified Longin method. *Radiocarbon*, 30, 171-177.
6. Stuiver, M and Polach, H. A. 1977. Discussion: Reporting of  $^{14}\text{C}$  Data. *Radiocarbon* 19: 355-363.
7. Wood, R.E., Bronk Ramsey, C. and Higham, T.F.G. 2010. Refining the ultrafiltration bone pretreatment background for radiocarbon dating at ORAU. *Radiocarbon* 52, Nr 2–3, 2010, p 600–611.
8. Bronk Ramsey, C. 2009. Bayesian analysis of radiocarbon dates. *Radiocarbon*, 51(1), 337-360.
9. Reimer, P.J. et al. 2009. Intcal09 and Marine09 radiocarbon age calibration curves, 0–50,000 years cal BP. *Radiocarbon* 51(4): 1111-1150.
10. Bronk Ramsey, C. 2009b. Dealing with outliers and offsets in radiocarbon dating. *Radiocarbon*, 51(3), 1023-1045.
11. Andersen, K.K. et al. 2006. The Greenland ice core chronology 2005, 15-42 ka. Part 1: constructing the time scale. *Quaternary Science Reviews*, 25(23-24), 3246-3257.
12. Weninger, B. and Jöris, O. 2008. A  $^{14}\text{C}$  age calibration curve for the last 60 ka: the Greenland-Hulu U/Th timescale and its impact on understanding the Middle to Upper Paleolithic. *Journal of Human Evolution* 55: 772–781.
13. Giaccio, B., Hajdas, I., Peresani, M., Fedele, F. G., Isaia, R., 2006, The Campanian Ignimbrite tephra and its relevance for the timing of the Middle to Upper Palaeolithic shift. In, Conard, N. J. (ed.) *When Neanderthals and Modern Humans Met*. Kerns Verlag: Tübingen, pp 343-375.

14. Moorrees, C F A, 1957. *The Aleut Dentition*. Massachusetts: Harvard Univ. Press, Cambridge.
15. Hillson, S, FitzGerald, C and Flinn, H. 2005 Alternative dental measurements: proposals and relationships with other measurements. *Am. J. Phys. Anth.* 126, 413-426.
16. Keith, A. 1927. Report on a fragment of a human jaw found at a depth of (10 1/2 ft) 3.2 m. in the cave earth of the vestibule of Kent's Cavern. *Trans Proc Torquay Nat Hist Soc* 5:1-2.
17. Frayer, D W, Jelinek, J, Oliva, M and Wolpoff, M H, 2006 Aurignacian male crania, jaws and teeth from the Mladeč Caves, Moravia, Czech Republic in Teschler-Nicola (Ed) *Early Modern humans at the Moravian Gate. The Mladeč Caves and their remains*. Springer Wien, NY, 185-272.
18. Wood, B A and Abbott, S A, 1983. Analysis of the dental morphology of Plio-Pleistocene hominids. I. Mandibular molars: crown area measurements and morphological traits. *J. of Anatomy*, 136, 1: 197-219.
19. Bermúdez de Castro, J M. et al. 2004. The Atapuerca sites and their contribution to the knowledge of human evolution in Europe. *Evolutionary Anthropology* 13, 1: 25-41.
20. Wolpoff, M H, 1979. The Krapina dental remains. *Am. J. Phys. Anth.* 50, 67-114.
21. Frayer, D W, 1978. *The evolution of the dentition in Upper Palaeolithic and Mesolithic Europe*. Kansas: University of Kansas, Publications in Anthropology number 10.
22. Sládek, V, Trinkaus, E, Hillson, S W & Holliday, T W, 2000. *The people of the Pavlovian: Skeletal Catalogue and Osteometrics of the Gravettian Fossil Hominids from Dolní Věstonice and Pavlov*. The Dolní Věstonice Studies, Vol 5. Vydal Archeologický ústav Akademie věd České republiky, Královopolská, 147, 612 00 Brno.

23. Rougier, H. et al. 2007 Peștera cu Oase 2 and the cranial morphology of early modern Europeans. *PNAS* 104, 4, 1165–1170.
24. Trinkaus, E, Milota, Ș, Rodrigo, R, Mircea, G and Moldovan, O, 2003b. Early modern human cranial remains from the Peștera cu Oase, Romania. *J. of Human Evolution* 45, 3, 245-253.
25. Black, G V, 1902. *Descriptive anatomy of the human teeth*, 4<sup>th</sup> ed. USA: S S White Dental Man. Co., Philadelphia.
26. Weidenreich, F, 1937. *The dentition of Sinanthropus pekinensis: a comparative odontology of the hominids*. Palaeontologia Sinica, whole series number 101, new series D,1.
27. Genet-Varcin E, 1975 Étude de dents humaines isolées provenant des grottes de la Chaise de Vouthon (Charante) III – Les Canines Supérieures. *Bull. et Mém. de la Soc. d'Anthrop. de Paris* t. 2, série XIII, 277-286.
28. Genet-Varcin E, 1976 Étude de dents humaines isolées provenant de la Chaise de Vouthon (Charante) IV – Les Prémolaires. *Bull. et Mém. de la Soc. d'Anthrop. de Paris* t. 3, série XIII, 243-259.
29. Lumley-Woodyear, M-A de, 1973 Anténéandertaliens et Néandertaliens du Bassin Méditerranéen Occidental Européen. *Études Quaternaires Mémoire No 2*, Université de Provence.
30. Martin, H, 1923. *L'homme fossile de la Quina* Archives de Morphologie, Librairie Octave Doin, Paris.
31. McCown, T, D and Keith, A, 1939. *The Stone Age of Mount Carmel II*. Oxford Clarendon Press.
32. NESPOS Database 2010 / [www.Nespos.org](http://www.Nespos.org)

33. Flécher, J P, Lefèvre, J and Verdène, J, 1976 Mensurations dentaires des hommes du Paléolithique Supérieur Français. *Bull. et Mém. de la Soc. d'Anthrop. de Paris* t. 3, série XIII, 383-400.
34. Bermúdez de Castro, J M, Rosas, A and Nicolás, M E, 1999. Dental remains from Atapuerca-TD6 (Gran Dolina site, Burgos, Spain). *J. of Human Evolution* 37, 3/4: 523-566.
35. Bailey S E. 2005. Diagnostic dental differences between Neandertals and Upper Paleolithic modern humans: Getting to the root of the matter. *Current Trends in Dental Morphology Research*. In Zadzińska E (Ed.) University of Lodz Press: Lodz (Poland), pp. 201-210.
36. Matiegka, J, 1934 *Homo Předmostensis – Fossilní Člověk z Předmostí Na Morarě I Lebky* Česká Akademie Věd a Umění, Prague.
37. Radovčić, J. (Ed). 1999. *The Krapina Hominids – a radiographic atlas of the skeletal collection* Croation NHM, Zagreb.
38. Skinner, M F, Sperber, G H and Tobias, P V, 1982 *Atlas of Radiographs of Early Man* Alan R Liss, New York.
39. Wheeler, R C, 1965. *A Textbook of Dental Anatomy and Physiology, 4<sup>th</sup> edition*. W B Saunders Co, London.
40. Beek, G C van, 1983. *Dental morphology, an illustrated guide, 2<sup>nd</sup> ed*. England: Wright, Bristol.
41. Trinkaus, E, 2007. European early modern humans and the fate of the Neandertals. *PNAS* 104, 18, 7367–7372.

42. Bilsborough, A and Thompson, J L, 2005. The Dentition of the Le Moustier 1 Neandertal. In Ullrich, H (Ed) *The Neandertal Adolescent Le Moustier 1 – new aspects, new results*, Staatliche Museum, Berlin: 157-186.
43. Patte, É, 1962. *La dentition des Néanderthaliens*. Masson et C<sup>ie</sup>, Paris.
44. Kallay, J. 1963. A radiographic study of the Neanderthal teeth from Krapina, Croatia in Brothwell, D R (Ed) *Dental Anthropology Symposia of the Society for the Study of Human Biology Vol 5*, Pergamon Press, Oxford, 75-86.
45. Oi, T, Saka, H and Ide, Y, 2004. Three-dimensional observation of pulp cavities in the maxillary first premolar tooth using micro-CT. *International Endodontic Journal* 37, 1, 46-51.
46. Bailey S E. 2004. A morphometric analysis of maxillary molar crowns of Middle-Late Pleistocene hominins *J. of Human Evolution* 47, 183-198.
47. Gómez-Robles, A. et al. 2007. A geometric morphometric analysis of hominin upper first molar shape. *J. of Human Evolution* 53, 272-285.
48. Day, M H, 1986. *Guide to fossil man, 4<sup>th</sup> ed*. Illinois: Univ. of Chicago Press.
49. Stringer, C B, Hublin, J J and Vandermeersch, B, 1984. The origin of anatomically modern humans in western Europe. In Smith, F H and Spencer, F (eds) *The origins of modern humans – a world survey of the fossil evidence*. New York: Alan R Liss: 51-135.
50. Lebel, S and Trinkaus, E, 2002. Middle Pleistocene human remains from the Bau de L'Aubesier. *J. of Human Evolution* 43: 659-685.
51. Trinkaus, E. et al. 2003. Later Middle Pleistocene human remains from the Almonda karstic system, Torres Novas, Portugal. *J. of Human Evolution* 45: 219-226.

52. Hillson S W and Coelho J M S 2002 The Dental Remains in Zilhão J and Trinkaus E (eds) *Portrait of the Artist as a Child, the Gravettian Human Skeleton from the Abrigo do Lagar Velho and its Archaeological Context* *Trabalhos de Arqueologia* 22, Instituto Português de Arqueologia, Lisboa, 342-355.
53. Barroso Ruiz, C., 2003. El Pleistoceno Superior de la Cueva del Boquete de Zafarraya. Junta de Andalucía. Consejería de Cultura, Sevilla.
54. Quam, R. et al. 2001. Human remains from Valdegoba cave (Huérmeces, Burgos, Spain). *J. Hum. Evol.* 41, 385-435.
55. Daura, J. et al. 2005. A Neandertal mandible from the Cova del Gegant (Sitges, Barcelona, Spain) *J. of Human Evolution*, 49, 1, 56-70.
56. Dumančić, J, Kaić, Z and Petrovečki, M. 2001 Evaluation of taurodontism in Krapina Neanderthals in Brook, A (Ed) *Dental Morphology 2001* 12<sup>th</sup> International Symposium on Dental Morphology, Sheffield Academic Press, UK, 111-121.
57. Irish, J D and Guatelli-Steinberg, D 2003. Ancient teeth and modern human origins: an expanded comparison of African Plio-Pleistocene and recent world dental samples. *J. of Human Evolution* 45, 113-144.
58. Vandermeersch, B, 1981. *Les Hommes Fossiles de Qafzeh (Israël)* Cahiers de Paléontologie, CNRS, Paris.
59. Schwartz, J H and Tattersall I, 2002. *The Human Fossil Record Vol 1 Terminology and Craniodental Morphology of Genus Homo (Europe)* Wiley-Liss, New York.
60. Coppa, A, Cucina, A, Vargiu, R, Manchinelli, D and Lucci, M, 2000 The Pleistocene Holocene transition in Italy. The evidence of morphological dental traits. In: Guarino, A. (ed.) *Proceedings, 2nd International Congress on 'Science and Technology*

*for the Safeguard of Cultural Heritage in the Mediterranean Basin, Nanterre, Paris, 5–9 July 1999*, Elsevier, Amsterdam. 1009-1013.

61. Drusini, A G, Toso, O and Ranzato, C, 1997. The Coronal Pulp Cavity Index: A Biomarker for Age Determination in Human Adults. *Am. J. Phys. Anth.* 103, 353–363.

62. Philippas, G.G. and Applebaum, E. 1968. Age Change in the Permanent Upper Canine Teeth. *J. Dental Research* 47, 411-417.

63. Deutsch A S, Musikant B L, Gu S and Isidro M, 2005. Morphological Measurements of Anatomical Landmarks in Pulp Chambers of Human Maxillary Furcated Bicuspid. *J of Endodontics*, 31, 8, 570-573.

64. Radovčić, J, Smith, F H, Trinkaus, E and Wolpoff, M H, 1988. *The Krapina hominids. An illustrated catalog of skeletal collection*. Croatia: Croatian Natural History Museum, Zagreb.

65. Trefný, P, 2005. Size reduction of the Le Moustier 1 molars – a 2D analysis. In Ullrich, H (Ed) *The Neandertal adolescent Le Moustier 1 – new aspects, new results*. Staatliche Museum, Berlin: 187-196.

66. Spoor, F., Zonneveld, F.W. and Macho, G.A. 1993. Linear measurements of cortical bone and dental enamel by computer tomography: applications and problems. *Am J Phys Anthropol* 91: 469-484.

67. Browning, B.L. 1969. *Analysis of Paper* (1st edition) New York: Marcel Dekker, Inc.

68. Williams, R. S. 1993. The Beilstein Test: Screening Organic and Polymeric Materials for the Presence of Chlorine, with Examples of Products Tested. *CCI Notes 17/1*. Canadian Conservation Institute. 1993. 3 pp. Wolpoff, M H, 1979. The Krapina dental remains. *Am. J. Phys. Anth.* 50: 67-114.



69. Koob, S. 1986. The use of Paraloid B-72 as an adhesive: Its application for archaeological ceramics and other materials. *Studies in Conservation* 31: 7-14.
70. Svensson, E.M, Anderung, C, Baubliene, J, et al. 2007. Tracing genetic change over time using nuclear SNPs in ancient and modern cattle. *Animal Genetics* 38, 378-383.
71. Krings, M. et al. 1997. Neandertal DNA sequences and the origin of modern humans. *Cell* 90: 19-30.
72. Compton, T and Stringer, C B 2011. The Human Remains. In Aldhouse-Green, S, Peterson, R and Walker, E A. (Eds) *Neanderthals in Wales: Pontnewydd and the Elwy Valley Caves*. Oxbow Books, Oxford
73. Condemi, S, 1992. *Les Hommes Fossiles de Saccopastore et leurs relations phylogénétiques*. Cahiers de Paléanthropologie, CNRS, Paris
74. Genet-Varcin E, 1975 Étude de dents humaines isolées provenant des grottes de la Chaise de Vouthon (Charante) III – Les Canines Supérieures. *Bull. et Mém. de la Soc. d'Anthrop. de Paris* t. 2, série XIII, 277-286.
75. Genet-Varcin E, 1976 Étude de dents humaines isolées provenant de la Chaise de Vouthon (Charante) IV – Les Prémolaires. *Bull. et Mém. de la Soc. d'Anthrop. de Paris* t. 3, série XIII, 243-259.
76. Villa, G and Giacobini, G, 1996. Neanderthal teeth from Alpine caves of Monte Fenera (Piedmont, Northern Italy).Description of the remains and microwear analysis. *Anthropologie (Brno)* 34, 1-2, 55-67
77. Genet-Varcin E, 1966. Étude de dents permanents provenant du gisement Moustérien de la Croze del Dua (Lot). *Annales de Paléontologie – Vertébrés* 52, 1, 87-114.

78. Hawkey, D E, 2003 Human Dental Remains from Gough's Cave (Somerset, England). *Bulletin Natural History Museum, London (Geology)* 58 (supp), 23-35.
79. Hillson, S W, 2006. Dental morphology, proportions, and attrition. In, Trinkaus, E and Svoboda, J (Eds) *Early Modern Human Evolution in Central Europe – the people of Dolní Věstonice and Pavlov* The Dolní Věstonice Studies Vol 12, Oxford University Press: 179-223.
80. Legoux, P. 1975. Présentation des dents des restes humains de L'Abri Pataud. In, Movius, H, L, (Ed) *Excavation of the Abri Pataud Les Eyzies (Dordogne)*. American School Prehistoric Research Bulletin No 30, Peabody Museum, Harvard University, Cam, Mass 262-305.
81. Legoux, P. 1976. Les dents de la Chaise de Vouthon – Etude pathologique et radiologique. *Bull. et Mém. de la Soc. d'Anthrop. de Paris* t. 3, série XIII, 345-361.
82. Sakura, H, 1979. Dentition of the Amud Man in Suzuki, H and Takai, F *The Amud Man and his Cave Site*, University of Tokyo, 207-230.
83. Schwartz, J H and Tattersall I, 2002b *The Human Fossil Record Vol 2 Terminology and Craniodental Morphology of Genus Homo (Africa & Asia)* Wiley-Liss, New York.
84. Trinkaus, E, 1983. *The Shanidar Neanderthals*. Academic Press, New York.

## Supplementary Figures and Legends

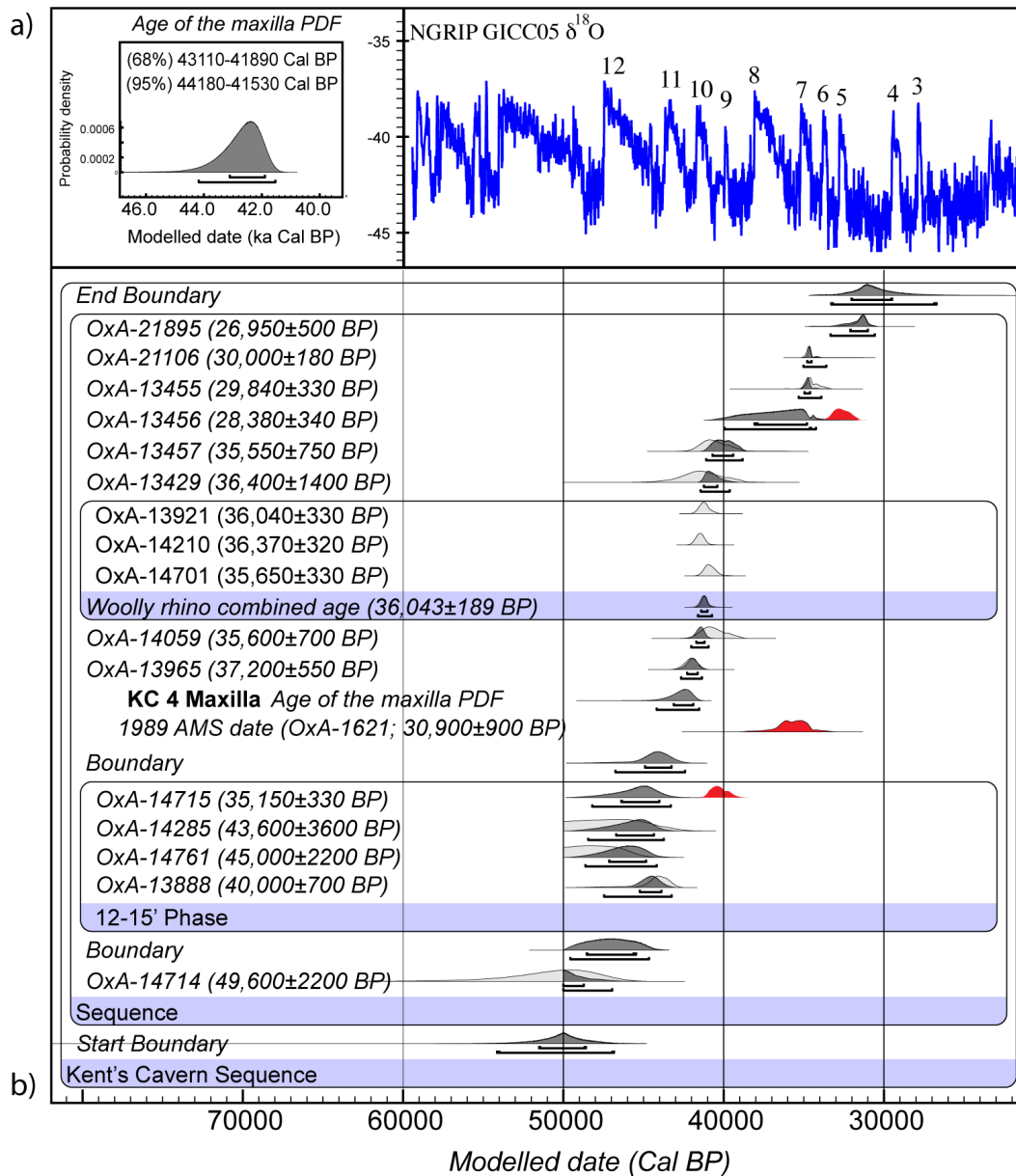


Figure S1: a) Kent's Cavern Bayesian model. This figure was made using OxCal 4.1<sup>8</sup>. Outliers in the model are highlighted in red, there are two. The original 1988 radiocarbon date of the maxilla (OxA-1621) is shown for illustrative purposes only also in red, and was not used in the modelling. You can note its much younger age than other dates above and below it. The radiocarbon dates are calibrated using the INTCAL09 curve<sup>9</sup> with resolution set at 20. The NGRIP  $\delta^{18}\text{O}$  record is shown, with Greenland

interstadials (GI) given where relevant<sup>1</sup>. The ice core record is tuned to the Hulu Cave chronology<sup>12</sup>. See text for details of the model. Individual likelihoods are shown with lighter shaded distributions. Posterior probability distributions are in black outline. Three woolly rhinoceros determinations were treated as coeval since they are either dates of the same bone, or dates of articulating bones. The determinations pass a chi-squared test ( $T'=2.4$ ,  $\chi^2=6.0$ , d.f.=2, 0.05 prob.). b) The posterior density function (PDF) ‘Age of the maxilla’ is shown in inset. This is an estimate for the likely age of the human maxilla (KC4) and not a direct date. It is important to note that the limit of the INTCAL09 calibration curve is 50,000 cal BP. OxA-14714 is not able to be calibrated due to this limit and instead is represented as a calendar date correlating to  $49500 \pm 2200$  cal BP. The determinations younger than this are calibrated directly against INTCAL09.

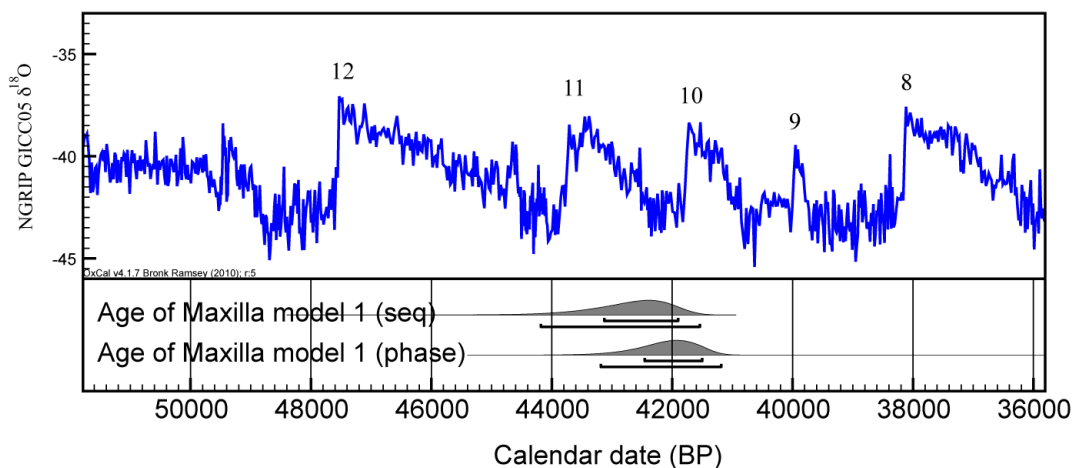


Figure S2: PDFs for the date function corresponding to the age of the maxilla. The Model 1 PDF results from modelling with the uppermost dates in sequence order, whilst the Model 2 PDF is produced when those dates are treated as an unordered phase. We prefer Model 1, and this is shown in Figure S1. The PDF is generated on the assumption

that the maxilla is in its original findspot with respect to depth above and below the other dated bones. For details of the NGRIP ice core data also shown, refer to the Figure S1 caption.

Neanderthal (Krapina)



Kent's Cavern



Modern human (recent)



L&lt;—&gt;B

Figure S3: Upper canine root shape (see text for details).

Neanderthal (Krapina)

Kent's Cavern

Modern human (recent)



Figure S4: Upper first premolar buccal angle

Neanderthal (Krapina)

Kent's Cavern

Modern (Gough's Cave)

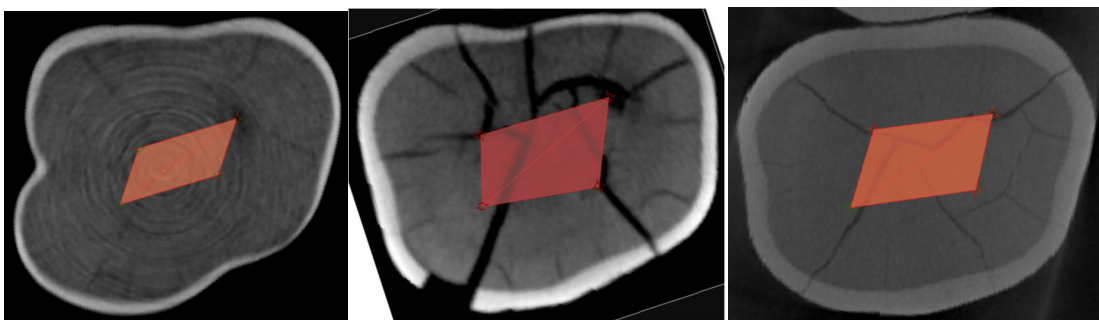
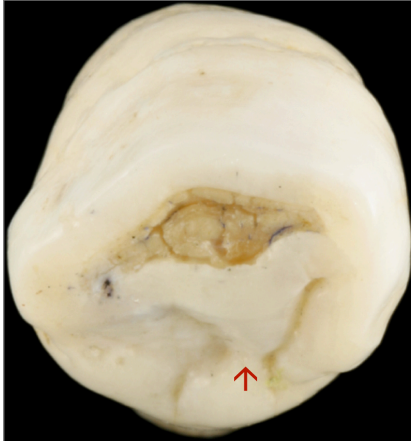


Fig. S5: Molar pulp chamber polygons

Neanderthal (Krapina)

Kent's Cavern



D<—>M

Figure S6 Upper canine tubercle extensions

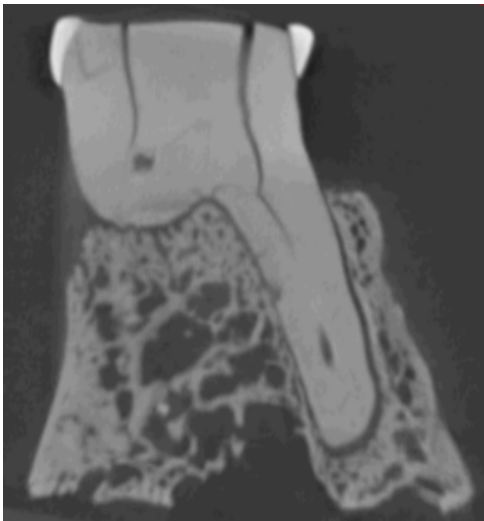


Figure S7: Kent's Cavern upper molar lingual roots

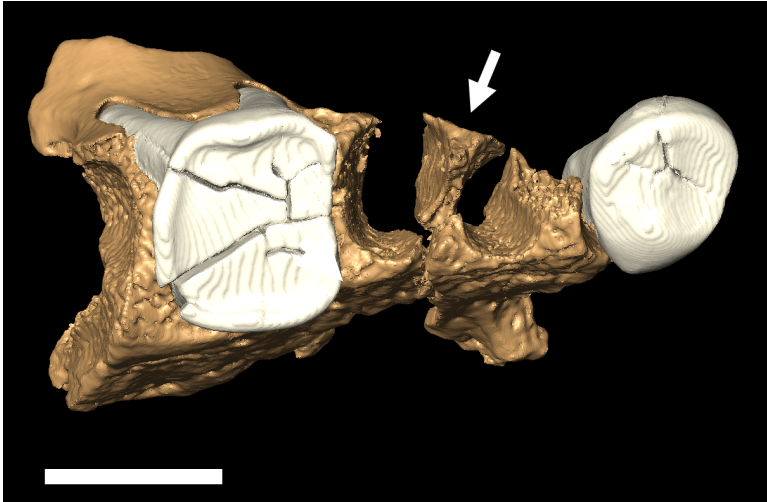


Figure S8: Superior view of the CT-based model. The premolar has been made invisible to show that the distal wall of the P<sup>3</sup> socket is part of a fragment that was glued to the specimen in a displaced position (white arrow). Note: scale bar = 1 cm.



Figure S9: Reconstruction of the maxilla.



## Supplementary Tables

Table S1: AMS radiocarbon determinations for human and animal bones from Trench C excavated in the Vestibule of Kent's Cavern, Devon in 1926-1928. Depths are measured from the assumed former position of the Holocene Granular Stalagmite. A thin stalagmite or breccia separates the sediments and the bones at 8'-0. \* Indicates repeat measurements on the same specimen. All are ultrafiltered gelatin determinations with the exception of OxA-1621. Stable isotope ratios are expressed in ‰ relative to vPDB. Mass spectrometric precision is  $\pm 0.2\%$ . Wt. used is the amount of bone pretreated and the yield represents the weight of gelatin or ultrafiltered gelatin in milligrams. %yield is the wt.%collagen which should not be  $< 1\text{wt.}\%$  at ORAU. This is the amount of collagen extracted as a percentage of the starting weight. %C is the carbon present in the combusted gelatin. For ultrafiltered gelatin this averages  $41.0 \pm 2\%$ . CN is the atomic ratio of carbon to nitrogen. At ORAU this is acceptable if it ranges between 2.9—3.5. Radiocarbon samples are given in depth below the granular stalagmite.

OxA	Context	Material	Species	Date	+/-	Used	Yield	%Yld	%C	$\delta^{13}\text{C}$	CN
21895	Vestibule 3'-4'.0	tooth	NHM E.86 Bone pin	26950	500	126	1.41	1.1	46.2	-21.0	3.5
21106	C4'-4''—4'-8''	tooth	<i>C.elaphus</i> , left M <sup>1</sup>	30000	180	1770	26.6	1.5	43.5	-18.0	3.4
13455	C5'-0	bone	<i>Canis lupus</i> left astragalus	29840	330	280	9.2	3.3	45.5	-19.2	3.4
13456	C5'-9''	tooth	<i>cf.Panthera leo</i> , canine fragment	28380	340	280	7.2	2.6	47	-19.9	3.4
13457	C7'-3''	bone	<i>Cervus elaphus</i> partial right dentary	35550	750	380	8	2.1	45.4	-19.3	3.4
13921	C8'-3''	bone	<i>Coelodonta antiquitatis</i> rt. Metacarpal 3	36040	330	560	31.1	5.6	36.7	-19.8	3.3
14210*	C8'-3''	bone	<i>Coelodonta antiquitatis</i> right metacarpal 4	36370	320	620	37.4	6	44.6	-20.1	3.3
14701*				35650	330	552	32	5.8	43.7	-19.4	3.3
14059	C9'-0	tooth	<i>Ursus arctos</i> left dentary	35600	700	480	8.4	1.8	41.7	-19.0	3.2

13965	C9'-6"	bone	<i>Coelodonta antiquitatis</i>	37200	550	580	15.05	2.6	40.2	-20.1	3.2
			cranial fragment								
1621	C10'-6"	bone	Human (1989 determination)	30900	900	500	8.7	1.7	17.2	-26.0	nd
14715	C12'-13'-0	bone	<i>Coelodonta antiquitatis</i>	35150	330	704	24.2	3.4	41.8	-19.4	3.3
			distal right tibia: heated								
14285	C13'-3"	tooth	<i>Panthera leo</i> , Left upper C	43600	3600	960	4.2	0.4	54.2	-17.4	3.2
14761	C14'-0	bone	<i>Coelodonta antiquitatis</i>	45000	2200	503	8.5	1.7	42	-19.9	3.4
			Left unciform								
13888	C15'-0	bone	<i>Rangifer tarandus</i> partial left dentary	40000	700	580	16.1	2.8	41.9	-18.5	3.3
14714	C19'-20'-0	bone	<i>Rangifer tarandus</i>	49600	2200	537	16.8	3.1	40.3	-18.6	3.3
			proximal right radius								

Table S2: Collagen yields from the KC4 redating attempt. As stated in the text, the sample was too low in collagen to allow a direct date.

Sample	Material	Species	Used (mg)	Yield (mg)	%Yld
KC 4	Tooth	<i>Homo</i> : right P <sup>3</sup>	89.0	0.38	0.4

Table S3: Kent's Cavern KC4 dental measurements

Upper permanent teeth (measurements in mm)										
Measurement	Direction	Right canine			Right third premolar			Right first molar		
		CT-scan	Frayer	Keith	CT-scan	Frayer	Keith	CT-scan	Frayer	Keith
Crown	MD length	7.9	7.9	7.2	7.25	6.9	7.0	10.3	9.8	10.0
	MD corrected	8.1	8.1	7.4	7.65	7.3	7.4	11.1	10.6	10.8

	BL Breadth	10.2	9.6	9.0	9.6	9.1	9.5	12.3	11.8	11.6
	Area (MDxBL)	83	78	67	73	66	70	137	125	125
	Index (BL/MD)	126	119	122	125	125	128	111	111	107
Root robusticity	MD	6.4		6.0	4.8		5.0	8.3		8.4
	BL	9.1			7.9			11.7		
	MDxBL	58			38			97		
Cervical	MD	6.3			4.9			8.9		
	BL	9.4			8.5			11.5		
	DB-ML							12.2		
	DL-MB							12.3		
Crown height		6.5		7.0	4.95		5.2	3.4		4.0
Root length	B/MB	17.7		16.5	16.8		16.2	14.8		
	DB							13.7		
	L	18.1						15.8		
Root trunk length	B							5.0		

M	5.8
D	5.8

Table S4: Crown comparative measurements

Sample	Upper canine					Upper third premolar					Upper first molar					
	N	Length (MD) mm	Breadth (BL) mm	Crown AREA	Crown INDEX	N	Length (MD) mm	Breadth (BL) mm	Crown AREA	Crown INDEX	N	Length (MD) mm	Breadth (BL) mm	Crown AREA	Crown INDEX	
<b>Atapuerca-SH</b>	Mean	17	8.6	9.7	83	113	13	8.0	10.7	86	134	16	11.1	11.5	128	104
	Range		8.1 - 9.6	8.8 - 10.7			7.2 - 8.9	9.7 - 11.8			9.9 - 12.3	10.3 - 13.0				
	SD		0.3	0.5			0.5	0.6			0.6	0.7				

<b>Krapina</b>	Mean	14	9.2	10.3	95	112	9	8.5	11.2	96	132	9	12.4	12.6	157	101
	Range		8.2 -	9.5 -	81 -	101 -		8.05 -	10.25 -	84 -	124 -		11.3 -	11.3 -	128 -	95 - 109
			10.0	11.4	114	131		9.3	11.8	109	139		13.6	14.2	185	
	SD		0.5	0.6	9	7		0.4	0.5	8	5		0.8	1.0	21	3
<b>Late</b>	Mean	13	8.2	9.6	79	119	11	7.4	10.5	77	141	17	11.2	12.0	136	109
<b>Neanderthals</b>	Range		6.65 -	8.4 -	62 - 95	106 -		6.5 -	9.2 - 11.5	64 - 96	119 -		10.0 -	10.4 -	120 -	99 - 130
			9.0	11.2		168		8.7			169		12.5	13.0	159	
	SD		0.7	0.7	10	16		0.6	0.6	9	13		0.8	0.7	11	9
<b>Kent's cavern</b>			7.4	9.0	67	122		7.4	9.5	70	128		10.8	11.6	125	107
<b>KC4</b>																
<b>Early Upper</b>	Mean	15	8.1	9.2	74	113	18	7.3	9.7	71	134	27	10.8	12.3	134	114
<b>Palaeolithic</b>	Range		7.1 -	7.75 -	55 - 98	101 -		5.9 -	8.7 - 10.6	54 - 84	112 -		9.1 -	11.0 -	102 -	107 -
			9.1	10.8		124		8.0			159		12.4	14.1	174	133
	SD		0.5	0.9	11	7		0.6	0.6	9	10		0.8	0.8	17	5

<b>Recent</b>	Mean	7.6	8.0	61	105	7.2	9.1	66	126	10.7	11.8	126	110
<b>European</b>	Range	7.0 -	7.0 -			7.0 -	8.0 - 10.0			9.0 -	11.0 -		
		9.0	9.0			8.0				12.0	12.0		

Notes: Late Neanderthal specimens consisted of: Gibraltar, Marina de Camerota, La Chapelle, La Croze, Le Moustier, La Quina, Meridionale, Palomas, Arcy-sur-Cure, La Ferrassie, Jersey, Kůlna, Monsempron, Pech de l'Azé, Spy, Teshik-Tash

Early Upper Palaeolithic specimens included: Brno, Cro-Magnon, Dolní Věstonice, Fontéchevade, Grotte des Enfants, Isturitz, Mladeč, Muierii, Oase, Předmostí, La Rochette, Les Rois.

Table S5: Crown measurements - relative tooth dimensions

Sample	UC % OF UP3		UC % OF UM1		UP3 % OF UM1	
	Length	Breadth	Length	Breadth	Length	Breadth
	(MD)	(BL)	(MD)	(BL)	(MD)	(BL)



<b>Late Neanderthals</b>	Mean	109	93	74	82	68	87
	Range	100 - 124	80 - 102	63 - 83	73 - 91	62 - 82	72 - 93
	SD	7	7	7	5	6	6
	Number	9	10	8	9	9	10
<b>Kent's Cavern KC4</b>		100	95	69	78	69	82
<b>Early Upper Palaeolithic</b>	Mean	110	93	75	75	68	80
	Range	95 - 136	82 - 102	65 - 83	67 - 81	59 - 78	69 - 85
	SD	10	5	5	5	5	3
	Number	14	14	14	14	16	18

Table S6: Cervical comparative measurements

Sample		Upper canine					Upper third premolar					Upper first molar				
		N	L	B	C	CI	n	L	B	C	CI	n	L	B	C	CI
<b>Neanderthals</b>	Mean	18	6.4	9.1	59	144	15	5.9	9.7	57	164	13	9.1	10.6	97	116
	Range		5.1 -	7.3 -	38 - 71	125 -		5.0 - 6.7	8.4 -	44 -	133 -		8.4 -	8.5 -	76 -	93 -
			7.3	10.5		166			11.0	69	195		10.6	11.8	111	135
	SD		0.7	0.8	10	12		0.4	0.9	7	18		0.7	1.0	10	15
<b>Kent's cavern</b>			6.3	9.4	59	149		4.9	8.5	42	173		8.9	11.5	102	129
<b>KC4</b>																
<b>Upper</b>	Mean	10	6.1	8.5	51	143	13	5.3	8.5	45	161	21	8.7	11.1	97	130
<b>Palaeolithic</b>																

Range	5.2 -	7.4 -	40 - 60	128 -	4.3 - 6.4	7.5 -	32 -	133 -	7.7 -	9.8 -	81 -	103 -
	6.9	9.6		160		9.8	54	188	10.0	13.2	132	141
SD	0.5	0.6	6	14	0.6	0.7	8	18	0.6	0.7	12	8

Notes: L = Length, B = Breadth, C = Cervical area, CI = Cervical Index. In millimetres.

Neanderthals included in this analysis are: Krapina, Le Petit Puymoyen, Montmaurin, Monsempron, Palomas, La Quina, Spy, Vindija

Upper Palaeolithic: Aurensan, Badegoule, Brassempouy, Cro-Magnon, Dolní Věstonice, Farincourt, Gough's Cave, Gourdan, Isturitz, La Chevre,

Laugerie-Basse, Le Placard, Les Rois, Lussac Les Châteaux, Lagar Velho, Muierii, Pataud, Pavlov, St Germain La Rivière, Vindija

Table S7: Cervical measurements - relative tooth dimensions

Sample		UC % of UP3		UC % of UM1		UP3 % of UM1	
		Length	Breadth	Length	Breadth	Length	Breadth
		(MD)	(BL)	(MD)	(BL)	(MD)	(BL)
Neanderthals	Mean	112	97	77	85	66	88
	Range	106 - 118	87 - 113	70 - 83	77 - 91	60 - 74	78 - 97

	SD	5	8	5	6	5	7
	Number	8	9	4	4	7	8
<b>Kent's Cavern KC4</b>		129	111	71	82	55	74
<b>Upper Palaeolithic</b>	Mean	124	106	74	80	60	76
	Range	104 - 138	88 - 121	68 - 78	74 - 90	52 - 67	71 - 83
	SD	10	12	4	6	6	5
	Number	9	6	4	5	8	10

Table S8: Percentage ratios of cervical to crown dimensions

Sample	Upper canine		Upper third premolar		Upper first molar	
	Length (MD)	Breadth (BL)	Length (MD)	Breadth (BL)	Length (MD)	Breadth (BL)

<b>Neanderthals</b>	Mean	74	95	73	90	77	91
	Range	64 - 84	89 - 104	68 - 83	83 - 98	65 - 89	82 - 97
	SD	6	4	5	5	7	4
	Number	16	17	14	17	12	12
<b>Kent's Cavern KC4</b>		85	104	66	89	82	99
<b>Upper Palaeolithic</b>	Mean	79	95	75	88	82	93
	Range	69 - 89	87 - 105	67 - 90	81 - 99	72 - 95	85 - 100
	SD	6	5	7	5	5	4
	Number	10	9	14	13	19	23

Table S9: Root robusticity - comparative measurements

Tooth	Identity	Root Robusticity sq. mm
<b>Upper canine</b>	' <i>Sinanthropus</i> ' n=6 mean (SD, range)	80 (14, 70-98)
	Atapuerca AT6	55
	Krapina n=9 mean (SD, range)	63 (8, 54-74)
	Other Neanderthals n=15 mean (SD, range)	54 (11, 32-87)
	Kent's Cavern KC4	58
	Upper Palaeolithic n=16 mean (SD, range)	49 (10, 37-72)
	Recent mean	44.5
<b>Upper third premolar</b>	' <i>Sinanthropus</i> ' n=4 mean (SD, range)	76 (17, 57-91)
	Krapina n=8 mean (SD, range)	63 (6, 55-69)

	Other Neanderthals n=7 mean (SD, range)	53 (10, 44-67)
	Kent's Cavern KC4	38
	Upper Palaeolithic n=15 mean (SD, range)	41 (4, 34-48)
	Recent mean	42.5
<b>Upper first molar</b>	' <i>Sinanthropus</i> ' n=5 mean (SD, range)	99 (10, 93-117)
	Atapuerca AT16, AT20	94 / 110
	Krapina n=9 mean (SD, range)	110 (18, 92-135)
	Other Neanderthals n=4 mean (SD, range)	99 (12, 86-114)
	Kent's Cavern KC4	97
	Upper Palaeolithic n=20 mean (SD, range)	90 (7, 78-108)
	Recent mean	81

Notes: Neanderthal specimens used: La Chaise de Vouthon, Hortus, Le Moustier, Palomas, La Quina, Tabun, Spy

Upper Palaeolithic: Mladeč, Ohalo, Gough's Cave, Aurenian, Bedeilhac, Bruniquel-Les Forges, Bruniquel-La Faye, Cheix, Cro-Magnon, Fontéchevade, Grimaldi, Isturitz, Laugerie-Basse, Pataud, Le Peyrat, Roc de Cave, Roc de Sers, Rochereil, Les Rois, Saint Germain la Rivière, Les Vachons, Veyrier

Table S10: Root lengths - comparative measurements

Tooth	Identity	Length
		mm
Upper canine	Gran Dolina Hominid 1	18.0
	' <i>Sinanthropus</i> ' mean & range, n = 4	22.6 (21.8-23.2)
	Atapuerca-SH AT6	19.9



	Neanderthals	mean & range, n = 15	22.0 (18.1-26.2)		
	Kent's Cavern KC4		18.1		
	Upper Palaeolithic	mean & range, n = 4	14.4 (12.5-16.0)		
	Předmostí	mean & range, n = 4	15.7 (12.5-19.7)		
	Recent European	mean & range	17.3 (11.0-20.5)		
<b>Upper third premolar</b>	Gran Dolina Hominid 1		16.9		
	' <i>Sinanthropus</i> '	mean & range, n = 2	20.2 (20.0-20.4)		
	Neanderthals	mean & range, n = 11	16.8 (14.1-19.6)		
	Kent's Cavern KC4		16.8		
	Upper Palaeolithic	mean & range, n = 4	13.8 (10.2-18.0)		
	Předmostí	mean & range, n = 4	13.1 (10.4-15.0)		
	Recent European	mean & range	12.4 (10.0-14.0)		
				<b><u>Mesiobuccal</u></b>	<b><u>Distobuccal</u></b>
				<b>mm</b>	<b>mm</b>
					<b><u>Lingual</u></b>
					<b>mm</b>

<b>Upper first molar</b>	Gran Dolina Hominid 1			15.8 / 16.1
	' <i>Sinanthropus</i> '	mean & range, n = 4		14.7 (13.7-15.4)
	Atapuerca-SH AT16	15.2	15.4	15.5
	Atapuerca-SH AT20		13.1	14.7
	Neanderthals	mean & range, n = 7		15.5 (12.5-18.4)
	Kent's Cavern KC4	14.8	13.7	15.8
	Upper Palaeolithic	mean & range, n = 2		12.3 (12.2-12.4)
	Předmostí	mean & range, n = 5		13.5 (11.4-16.4)
	Recent European	mean & range		13.2 (10.0-16.0)

Table S11: Samples for morphological comparisons - sources

NEANDERTHALS		UPPER PALAEOLITHIC (EARLY MODERN <i>HOMO SAPIENS</i> )	
SITE	REFERENCE	SITE	REFERENCE
Amud Cave	Sakura 1979 <sup>82</sup> , cast	Abri Pataud	Legoux 1975 <sup>80</sup> , Schwartz and Tattersall 2002 <sup>59</sup>
La Chaise de Vouthon	NESPOS <sup>32</sup> , Genet-Varcin 1975 & 1976 <sup>74,75</sup> , Legoux 1976 <sup>81</sup>	Barma Grande	Schwartz and Tattersall 2002 <sup>59</sup>
La Chapelle-aux-Saints	Lumley-Woodyear 1973 <sup>29</sup>	Brno	Cast
La Croze del Dua	Genet-Varcin 1966 <sup>77</sup>	Combe Capelle	Cast
Engis	NESPOS <sup>32</sup>	Cro-Magnon	Cast
La Ferrassie	Cast	Dolní Věstonice	Hillson 2006 <sup>79</sup> , Schwartz and Tattersall 2002 <sup>59</sup>
Gibraltar	Casts	La Geniere	Cast

Hortus	Lumley-Woodyear 1973 <sup>29</sup>	Gough's Cave	Originals, Hawkey 2003 <sup>78</sup>
Krapina	NESPOS <sup>32</sup> , Radovčić 1999 <sup>37</sup> , Radovčić et al 1988 <sup>64</sup> , casts	Grotte des Enfants	Cast
Kůlna	Cast	Isturitz	Schwartz and Tattersall 2002 <sup>59</sup>
Marina de Camerota (Grotta Taddeo)	X-ray photographs taken by R L Tompkins	Ksar 'Akil	Cast
Monsempron	Lumley-Woodyear 1973 <sup>29</sup>	Lagar Velho	Hillson and Coelho 2002 <sup>52</sup>
Ciota Ciara (Monte Fenera)	Villa and Giacobini 1996 <sup>76</sup>	Mladeč	Frayner <i>et al</i> 2006 <sup>17</sup> , casts
Le Moustier	NESPOS <sup>32</sup> , Bilsborough and Thompson 2005 <sup>42</sup>	Nahal Ein Gev	Cast
La Quina	NESPOS <sup>32</sup> , Martin 1923 <sup>30</sup> , casts	Oase	Rougier <i>et al</i> 2007 <sup>23</sup>
Saccopastore	Condemi 1992 <sup>73</sup> , casts	Oberkassel	Cast
St Césaire	Cast	Ohalo	Cast
Sakajia	Cast	Parpalló	Skinner <i>et al</i> 1982 <sup>38</sup> , cast
Shanidar	Trinkaus 1983 <sup>84</sup> , casts donated by	Pavlov	Hillson 2006 <sup>79</sup>

E Trinkaus			
Spy	NESPOS <sup>32</sup>	Le Placard	Skinner <i>et al</i> 1982
Tabun Cave	McCown and Keith 1939 <sup>31</sup>	Předmostí	Matiegka 1934 <sup>36</sup> , casts
Teshik-Tash	Cast	Svitavka	Schwartz and Tattersall 2002 <sup>59</sup>
ARCHAIC <i>HOMO SAPIENS</i>			
SITE	REFERENCE		
Qafzeh	Schwartz and Tattersall 2002 <sup>83</sup> , Vandermeersch 1981 <sup>58</sup> , casts		
Skhūl	Schwartz and Tattersall 2002 <sup>83</sup> , McCown and Keith 1939 <sup>31</sup> , casts		

Table S12: Crown and root morphological features - comparative data

TOOTH	FEATURE	KRAPINA	OTHER NEANDERTHALS	ARCH <i>H</i> <i>SAPIENS</i>	UPPER PALAEOLITHIC	POUNDBURY
<b>Upper canine</b>	Mesiobuccal bulge	86% (12/14)	70% (21/30)	89% (8/9)	45% (10/22)	67% (12/18)
	Tubercle extensions	85% (11/13)	74% (14/19)	71% (5/7)	27% (3/11)	14% (2/14)

	Prominent tuberculum dentale	77% (10/13)	75% (18/24)	50% (4/8)	42% (5/12)	
	Vertical convexity of root	60% (6/10)	88% (15/17)	0% (0/3)	0% (0/5)	
	Surface of root granulated	0% (0/12)	62% (8/13)		0% (0/5)	
<b>Upper third premolar</b>	Mesiobuccal bulge	27% (3/11)	35% (9/26)	25% (2/8)	8% (2/25)	0% (0/17)

Table S13: Crown buccal surface angles(°) - comparative data

	UPPER CANINES					UPPER THIRD PREMOLARS				
	MEAN	NUMBER	SD	MAX	MIN	MEAN	NUMBER	SD	MAX	MIN
<b>Archaic <i>Homo sapiens</i></b>	31	4	2	34	30	24	4	7	35	18
<b>Krapina</b>	28	11	6	35	18	28	10	9	33 & one at 54	19
<b>Other Neanderthals</b>	23	22	5	34	15	26	18	4	34	21
<b>Kent's Cavern</b>	29					13				
<b>Upper Palaeolithic</b>	24	8	8	34	15	18	11	3	24	13
<b>Recent</b>	24	6	4	28	19	15.5	6	5	21	9

Table S14: Pulp chamber &amp; root canal dimensions (mms) - comparative data

UPPER CANINES												
	KRAPINA (n=5)			OTHER NEANDERTHALS (n=7)			KENT'S CAVERN	GOUGH'S CAVE (n=3)		RECENT (n=6)		
	MEAN	SD	RANGE	MEAN	SD	RANGE		MEAN	RANGE	MEAN	SD	RANGE
<b>Shape (ratio of mesiodistal to buccolingual widths)</b>												
- pulp chamber	0.57	0.17	0.38 - 0.77	0.52	0.12	0.42 - 0.78	0.37	0.42	0.40 - 0.47	0.56	0.08	0.46 - 0.69
- root canal at 1/3 from cervix	0.73	0.21	0.46 - 0.97	0.67	0.20	0.30 - 0.97	0.40	0.49	0.41 - 0.55	0.59	0.21	0.40 - 1.00
<b>Pulp chamber - buccolingual (max)</b>	3.4	0.5	2.7 - 4.0	3.1	0.4	2.6 - 3.8	3.1	3.2	3.2 - 3.3			

- mesiodistal (max)	1.9	0.3	1.4 - 2.2	1.6	0.5	1.3 - 2.6	1.15	1.4	1.3 - 1.5
Root canal - buccolingual (max)	3.3	1.0	2.6 - 4.9	2.9	0.7	2.2 - 4.2	3.2	3.8	3.5 - 3.9
- mesiodistal (max)	2.2	0.2	1.9 - 2.6	1.8	0.7	1.0 - 3.0	0.95	1.5	1.4 - 1.5
Cross-sectional area - pulp chamber (max)	4.4	0.7	3.8 - 5.4	3.9	2.0	2.4 - 7.3	2.35	2.9	2.6 - 3.3
- root canal at 1/3 from cervix	2.7	0.5	2.3 - 3.4	2.3	1.7	0.8 - 5.0	1.0	1.7	1.2 - 1.9

## UPPER THIRD PREMOLARS

	KRAPINA (n=4)			OTHER NEANDERTHALS (n=3)		KENT'S CAVERN	GOUGH'S CAVE (n=1)		RECENT (n=6)		
	MEAN	SD	RANGE	MEAN	RANGE		MEAN	RANGE	MEAN	SD	RANGE
Shape (ratio of mesiodistal to buccolingual widths)											
- pulp chamber	0.40	0.01	0.38 - 0.41	0.44	0.33 - 0.47	0.21	0.27		0.32	0.11	0.20 - 0.51



<b>- root canal before bifurcation</b>	0.35	0.06	0.30 - 0.45	0.45	0.42 - 0.48	0.23	0.31*	0.19	0.04	0.13 - 0.26
<b>Pulp chamber - buccolingual (max)</b>	5.0	0.3	4.6 - 5.3	4.7	3.6 - 5.3	3.3	3.7			
<b>- mesiodistal (max)</b>	1.9	0.2	1.6 - 2.2	2.1	1.4 - 2.5	0.7	1.0			
<b>Root canal before bifurcation - buccolingual</b>	4.0	0.5	3.2 - 4.5	3.9	2.9 - 5.0	3.05	2.2*			
<b>- mesiodistal</b>	1.4	0.1	1.3 - 1.5	1.8	1.3 - 2.1	0.7	0.7*			
<b>Pulp chamber cross-sectional area (max)</b>	6.7	1.3	5.5 - 8.1	6.5	3.7 - 8.5	2.0	2.3			
<b>Root canal cross-sectional areas</b>										
<b>- before bifurcation</b>	4.0	0.6	3.1 - 4.7	4.5	2.8 - 6.5	1.3	1.1*			
<b>- after first bifurcation -buccal</b>	1.1	0.3	0.8 - 1.6	1.7	0.8 - 3.0	0.4				
<b>- lingual</b>	1.2	0.2	0.9 - 1.4	1.3	0.7 - 1.8	0.3				
										RECENT (n=107)
<b>Height of pulp chamber roof - from cervix</b>	0.2	0.8	-0.6 - 1.1	0.9	0.6 - 1.2	1.65	1.0			

<b>- from bifurcation</b>	3.1	1.0	1.8 - 4.4	4.1	3.8 - 5.0	4.05	4.61	1.04
Neanderthals: La Chaise, Le Moustier, La Quina, Spy			*: Single root canal, measured at 4 mm from pulp chamber roof					

Table S15: Ratios of upper first molar cervical diagonal measurements (pr-met / par-hyp) - comparative data.

<b>SAMPLE</b>	<b>MEAN</b>	<b>NUMBER</b>	<b>SD</b>	<b>MAX</b>	<b>MIN</b>
<b>Archaic <i>Homo sapiens</i></b>	0.92	4	0.04	0.98	0.87
<b>Krapina</b>	0.86	13	0.03	0.90	0.81
<b>Other Neanderthals</b>	0.86	17	0.04	0.95	0.79
<b>Kent's Cavern</b>	0.99				
<b>Upper Palaeolithic</b>	0.89	15	0.03	0.94	0.82

<b>Recent (Poundbury)</b>	0.89	16	0.04	0.99	0.78
---------------------------	------	----	------	------	------

Table S16: Upper first molar pulp chamber polygons - comparative data

	<b>KRAPINA (n=6)</b>			<b>OTHER NEANDERTHALS (n=3)</b>		<b>KENT'S CAVERN</b>	<b>GOUGH'S CAVE (n=2)</b>	
	MEAN	SD	RANGE	MEAN	RANGE		MEAN	RANGE
<b>Angles (°) - Protocone</b>	121	5.3	115 - 128	125	116 - 135	108	111	102 - 121
- Paracone	58	4.1	51 - 63	63	58 - 71	68	68	62 - 74
- Metacone	121	4.8	115 - 129	108	107 - 112	104	105	101 - 109
- Hypocone	60	5.6	54 - 68	64	60 - 66	80	76	70 - 86
<b>Ratio of Diagonal Measurements</b>	0.60	0.035	0.54 - 0.63	0.65	0.61 - 0.70	0.77	0.76	0.74 - 0.79
<b>Ratios of polygon sides to total circumference</b>								
- Mesial (Protocone to Paracone)	0.30	0.015	0.28 - 0.32	0.31	0.29 - 0.32	0.34	0.33	0.30 - 0.37
- Buccal (Paracone to Metacone)	0.21	0.016	0.19 - 0.22	0.21	0.20 - 0.23	0.20	0.20	0.19 - 0.22
- Distal (Metacone to Hypocone)	0.30	0.018	0.27 - 0.32	0.31	0.29 - 0.32	0.30	0.31	0.31 - 0.32
- Lingual (Hypocone to	0.19	0.016	0.18 - 0.22	0.17	0.16 - 0.19	0.16	0.16	0.12 - 0.19

Protocone)								
<b>Ratio of polygon area to crown base area</b>	0.09	0.027	0.06 - 0.14	0.09	0.08 - 0.10	0.10	0.11	0.10 - 0.11
Neanderthals: Le Moustier, Spy, Engis								

Table S17: Reasons for change in identification of premolar from P<sup>4</sup> to P<sup>3</sup>

1. The distal interproximal facet does not match the mesial interproximal facet of the molar
2. The root does not fit well in the fourth premolar socket but appears (although the remains are fragmentary) to fit in the third premolar socket
3. The occlusal outline, with the buccal cusp being noticeably larger and wider than the lingual, suggests a third rather than a fourth premolar
4. There is a distinct canine groove on the mesial surface of the root and crown
5. The mesial interproximal facet exactly matches the distal interproximal facet of the canine.